

84/16
S 12
89/16

En 27

LA-6241-T

Thesis

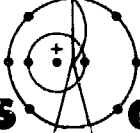
UC-45

Issued: February 1976

A Precipitation Model and Experimental Correlation with Various Properties of Pentaerythritol Tetranitrate

by

Thomas Rivera


los alamos
scientific laboratory
of the University of California

LOS ALAMOS, NEW MEXICO 87545

An Affirmative Action/Equal Opportunity Employer

UNITED STATES
ENERGY RESEARCH AND DEVELOPMENT ADMINISTRATION
CONTRACT W-7405-ENG. 36

This thesis was submitted to the University of New Mexico, Albuquerque, NM, in partial fulfillment of the requirements for the degree of Doctor of Philosophy in Chemistry. It is the independent work of the author and has not been edited by the Technical Information staff.

Printed in the United States of America. Available from
National Technical Information Service
U.S. Department of Commerce
5285 Port Royal Road
Springfield, VA 22151
Price: Printed Copy \$6.00 Microfiche \$2.25

This report was prepared as an account of work sponsored by the United States Government. Neither the United States nor the United States Energy Research and Development Administration, nor any of their employees, nor any of their contractors, subcontractors, or their employees, makes any warranty, expressed or implied, or assumes any legal liability or responsibility for the accuracy, completeness, or usefulness of any information, apparatus, product, or process disclosed, or represents that its use would not infringe privately owned rights.

CONTENTS

	<u>Page</u>
LIST OF FIGURES	iv
LIST OF TABLES	v
ABBREVIATIONS AND SYMBOLS	vi
ABSTRACT	ix
I. INTRODUCTION	1
II. OBJECTIVES	2
III. PROPERTIES OF PETN	3
IV. EBW DETONATORS	6
V. CRYSTALLIZATION THEORY	10
A. Plug Flow Model	10
B. Dispersed Plug Flow Model	15
C. Kinetics	18
D. Inversion of the Moments	20
E. Comparison of Theory with Experiment	21
VI. EXPERIMENTAL	24
A. Apparatus	24
B. Materials	29
C. Procedure	30
D. Particle Measurement	33
E. Detonator Test Firing	34
VII. RESULTS	37
A. Experimental Particle Size Distributions	37
B. Theoretical Model Predictions	48
C. Detonation Characteristics	58
VIII. CONCLUSIONS	61
APPENDIX A	53
APPENDIX B	66
ACKNOWLEDGMENTS	78
REFERENCES	79

NOTICE
This report was prepared as an account of work sponsored by the United States Government. Neither the United States nor the United States Energy Research and Development Administration, nor any of their employees, nor any of their contractors, subcontractors, or their employees, makes any warranty, express or implied, or assumes any legal liability or responsibility for the accuracy, completeness or usefulness of any information, apparatus, product or process disclosed, or represents that its use would not infringe privately owned right.

LIST OF FIGURES

<u>Figure</u>		<u>Page</u>
1.	Solubility of PETN in Aqueous Acetone Solutions	4
2.	PETN Crystallization Apparatus	24
3.	Static Mixer	26
4.	Cumulative logarithmic plot of photelometer analysis of HMX and of sieve analysis of coarse fraction above 45 μm	34
5a-f.	PETN Experimental Particle Size Distribution	38-40
6a-g.	PETN Scanning Electron Micrographs	41-47
7a-f.	Comparison of Theoretical Values with Experimental Particle Size Distributions	50-52
8.	Theoretical Kinetics Along Reaction Coordinate	56
9.	Growth Rate Kinetics Along Reaction Coordinate	56
10.	Variation of Moments Along Reaction Coordinate	57
11.	PETN Detonator Threshold Voltages	59
12.	PETN Detonator Transit Times	60

LIST OF TABLES

<u>Table</u>		<u>Page</u>
1	Experimental M_T Results	14
2	Experiment Holding Times and Flow Rates	28
3	Particle Size Characteristics	37
4	Calculated Kinetic Quantities	55
5	Correlation of Threshold Voltage with \bar{L}	59
6	Correlation of Transit Time with \bar{L}	60
7	Summary of Theoretical Equations	62

LIST OF SYMBOLS AND ABBREVIATIONS

<u>Symbol or Abbreviation</u>	<u>Explanation</u>
a	Nucleation rate parameter, constant
b	Growth rate parameter, constant
B^0	Nucleation rate (nuclei/cm ³ · s)
B_0^0	Initial nucleation rate (nuclei/cm ³ · s)
C_0	Initial concentration (g/cm ³)
C_s	Concentration of saturated solution (g/cm ³)
C. V.	Coefficient of variation
D	Axial diffusion coefficient
$E_{0.5}$	Threshold voltage (V)
EBW	Exploding bridgewire
f_j	jth dimensionless moment of the population
G	Growth rate ($\mu\text{m/s}$)
G_0	Initial growth rate ($\mu\text{m/s}$)
HMX	Octahydro-1, 3, 5, 7-tetranitro-s-tetrazocine
K	Constant
K_v	Volume shape factor, constant
L	Internal coordinate (μm or cm)
\bar{L}	Mass-weighted mean particle size (μm or cm)
m_j	jth moment of the population
M_r	Solids concentration (g/cm ³), clear liquid basis
n	Population density [number/(unit length)(unit slurry volume)]

List of Symbols and Abbreviation--contd.

<u>Symbol or Abbreviation</u>	<u>Explanation</u>
n^0	Nuclei population density [number/(unit length)(unit slurry volume)]
N	Number of crystals
Pe	Péclet number or diffusion parameter, constant
PETN	Pentaerythritol tetranitrate
R	Ratio of PETN-acetone solution flow rate to flow rate of water
RMC	Rotating mirror camera
t	Time (s)
t_m	Transit time (μ s)
u_x	Plug flow velocity (cm^3/s)
W	Weight distribution function
WW	Cumulative weight fraction distribution
x	External coordinate (cm)
\bar{x}	Effective reactor length (cm)
y	Dimensionless population density
z	Dimensionless external coordinate (reaction coordinate)
β	Dimensionless concentration
β_s	Dimensionless saturated concentration
ΔL	Width of crystal size range (μm or cm)
$\Delta \xi$	Dimensionless width of crystal size range
ρ	Particle density (g/cm^3)

List of Symbols and Abbreviations--contd.

<u>Symbol or Abbreviation</u>	<u>Explanation</u>
σ	Standard deviation
τ	Retention time (s)

A PRECIPITATION MODEL AND EXPERIMENTAL
CORRELATION WITH VARIOUS PROPERTIES OF
PENTAERYTHRITOL TETRANITRATE

Thomas Rivera, Ph. D.
Department of Chemistry
The University of New Mexico, 1975

ABSTRACT

A continuous precipitation method for the preparation of crystalline pentaerythritol tetranitrate (PETN) has been developed. The process involves the precipitation of PETN from an acetone solution by the addition of water in a static mixer. The principal independent variable is the ratio, R , of the acetone-PETN solution flow rate to the flow rate of water.

A mathematical model based on dispersed plug-flow equations adequately represents the physical process. The relationships developed can be used to predict particle size distributions, two explosion properties of PETN, and estimate the effective kinetics involved in the precipitation process. The mass-weighted mean particle size, \bar{L} , of the precipitated PETN is a linear function of R . The initial nucleation and growth rates are exponentially decaying functions of R . The nucleation exponent is 3.75 ± 0.05 ; the growth rate exponent is 1.56 ± 0.02 . The value of the diffusion parameter, Pe , is 51 ± 1 . Experimentally determined PETN initiation-threshold voltages can be expressed as a second degree polynomial in \bar{L} , with a minimum at about $50 \mu\text{m}$. Observed PETN explosion transit times follow a third degree polynomial in \bar{L} , increasing with increasing particle size.

I. INTRODUCTION

An important consideration in the applications of high explosives is the ability to predict the physical and explosion properties of the material. In the case of a crystalline explosive, the particle size distribution and crystal habit are important.^{11,20} Batch processes commonly used in the preparation of high explosives frequently result in large variations in the products³ and usually provide little information about the kinetics of the process. A method for the preparation of a reproducible crystalline product having a known particle size distribution and crystal habit is desirable.

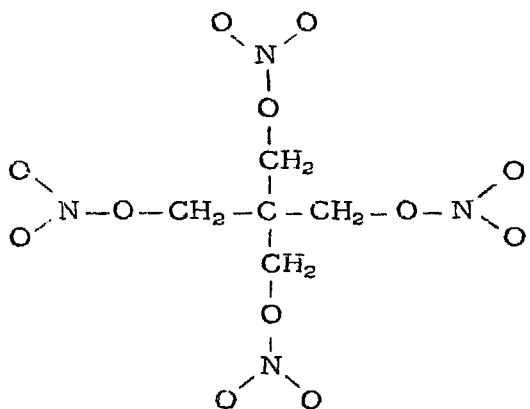
The method of recrystallization employed in this work involves the precipitation of PETN from an acetone solution by the addition of water in a static mixer. The primary independent variable is the ratio, R, of the PETN-acetone solution flow rate to the flow rate of water.

II. OBJECTIVES

The objectives of this study are to develop a continuous reproducible recrystallization technique for the preparation of the high explosive, pentaerythritol tetranitrate (PETN), which has definite crystalline properties, and to develop a model that provides some information on the kinetics and predicts the crystalline and explosion properties of the product.

III. PROPERTIES OF PETN

PETN is a symmetrical, nonpolar organic compound, $[C(CH_2ONO_2)_4]$, namely,



having a formula weight of 316.15. It forms colorless, nonhygroscopic crystals. PETN is readily compressible and has a maximum density of 1.77 g/cm³. It melts at 141°C and decomposes rapidly at temperatures above its melting point. PETN is insoluble in water, and soluble in acetone. Figure 1 gives the solubility of PETN in mixtures of acetone and water.¹⁹

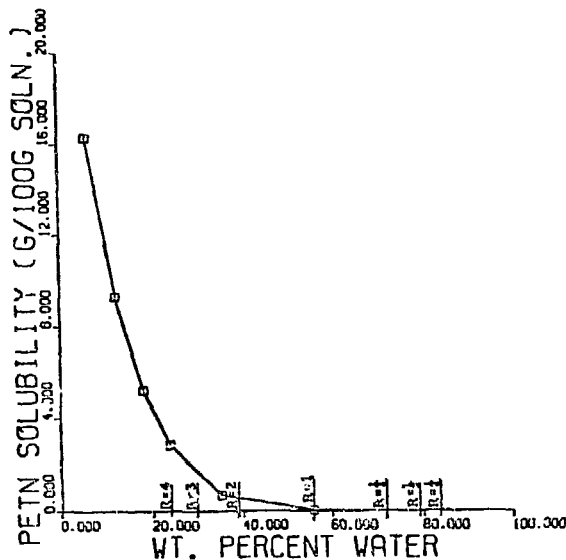
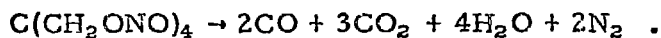


Figure 1.
Solubility of PETN in Aqueous Acetone Solutions.

PETN has an ignition temperature of approximately 215°C, which is slightly higher than that of nitroglycerin. It is of the same order of sensitivity to impact as nitroglycerin. PETN detonates or decomposes according to the equation



Its heat of detonation lies between 1466 and 1543 cal/g.¹ The high explosive strength of PETN has been attributed to the fact that its oxygen deficiency is small (10.1%). The decomposition products of the ideally oxygen-balanced material would be CO₂, H₂O, and N₂, without the formation of CO. The ability to compress PETN to a relatively high density is also a major contributing factor.

PETN has a detonation velocity of 5330 m/s for compacted material (density 0.85 g/cm³), 7600 m/s for material having a density of

1.5 g/cm³, and 8320 m/s for highly compressed material (density 1.70 g/cm³). The brisance or shattering power of PETN is much greater than that of nitroglycerin. Its explosive strength is at least 50% greater than TNT.⁵

Because of its great explosive power and brisance, PETN is widely used as a military and industrial explosive. Its ease of initiation and its high explosive power combine to make PETN exceptionally serviceable in detonators as the donor charge that initiates a less sensitive acceptor explosive. PETN has also been used in percussion caps and grenades and as a propellant in smokeless powders.^{1,5}

PETN can be used in the treatment of angina pectoris as a long-acting coronary vasodilator, which is capable of reducing the frequency and severity of the attack.¹

IV. EBW DETONATORS

Chemical explosives comprise two main types: (1) detonating or "high" explosives, characterized by very high rates of reaction and high pressures and (2) deflagrating or "low" explosives, which burn more slowly and develop much lower pressures. Detonating explosives may be further subdivided into (a) primary and (b) secondary explosives. Primary explosives nearly always detonate by simple ignition such as by a spark, flame, impact, or other primary heat sources of appropriate magnitude. Secondary explosives require, in practical applications, the use of a detonator and frequently, a booster. A booster is a sensitive secondary high explosive that reinforces the detonation wave from the primary explosive or detonator and delivers a more powerful detonation wave to the main explosive charge.³

A problem encountered in explosive operations is that of initiating the detonation wave in the explosive. Often, this problem is complicated by the provisions of simplicity and safety, and the necessity of precisely controlled timing at widely separated points. A variety of devices, called detonators, have been developed to perform the function of initiation. The exploding bridgewire (EBW) detonator has an explosive train with a secondary explosive requiring an elaborate power source to vaporize or "explode" a wire by extremely rapid deposition of electrical energy to initiate detonation in the material.²²

The basic circuit for exploding a wire consists of a power source to charge a capacitor, a capacitor for storage of electrical energy, a

spark gap and trigger switch to discharge the capacitor across the bridgewire, a transmission line to the bridgewire, and a bridgewire. As the switch is closed, voltage is applied to the transmission line and bridgewire circuit which causes current to begin to flow at a rate controlled by the RLC characteristics of the circuit. The rate of current flow (approximately $1000 \text{ A}/\mu\text{s}$) and the amount of energy are so great that the wire is heated to vaporization but the physical shape of the wire is maintained by inertia. As vaporization occurs, the resistance of the wire increases greatly. At this point, the current reduces within approximately one microsecond. Within a few nanoseconds after vaporization, the inertia of the wire material is overcome and the wire explodes giving off a shock wave and the contained thermal energy.¹⁸

The problem of finding a secondary explosive sufficiently sensitive to be initiated by the small shock developed by the exploding wire is resolved by utilizing an intrinsically sensitive secondary explosive. Generally, PETN loaded as a low density granular powder of controlled particle size and shape is used. Even though the effective sensitivity of secondary explosives may be increased by the proper selection of physical parameters, such materials are still 3 to 4 orders of magnitude less sensitive than primary explosives.²²

The basic inert components of an EBW detonator consist of a header that contains the electrical wire leads and the bridgewire. Header material may vary from plastic to a metal/ceramic combination. The electrical connection may be hookup wire leads or a coaxial

or multipin assembly into which the cable mates directly. The sleeve, which actually contains the explosive, may be a part of the header or a separate part that is threaded or crimped into place. End caps may be used. The explosive is generally pressed in two increments. The first increment, next to the bridgewire, is pressed into the header at a density of approximately 50% of that of the crystal density. The second increment, called the output charge, is pressed to approximately 90% of that of the crystal density.¹⁸

The shock wave and thermal energy released from the exploding bridgewire are transferred into the low density secondary explosive next to the bridgewire. In general, the shock wave from the wire travels at about 1500 m/s. As the wave travels into the explosive, a detonation of the explosive is initiated and builds up to the normal detonation velocity of the initial pressing explosive (approximately 5000 m/s). As the shock wave moves through the initial pressing and into the output pellet, the velocity of the wave again increases, because of the higher density pellet, to approximately 8000 m/s.¹⁸ The time from bridgewire burst to shock wave breakout is called the function or transit time of the detonator (t_m). This time is on the order of one to several microseconds, depending on the overall length of the detonator. Another quantity that is often used is the threshold voltage ($E_{0.5}$). The threshold voltage is the firing set capacitor voltage level at which one half of the detonators will fire.

EBW detonators are used for many applications including the following:¹⁸

- The production of accurate and refined metal forming or welding
- The generation of shock waves for physics research studies
- The creation of small point energy or light sources
- The closure of an electrical switch in a very short and predictable time.

V. CRYSTALLIZATION THEORY

The techniques for interpreting crystal size distributions from crystallization processes to ascertain the nature of the controlling mechanism developed rapidly over the period from 1962 to 1964²⁴ (Randolph and Larson,¹⁶ Hulbert and Katz¹⁰). The work began with the first attempts to rationalize, model, and predict crystal size distributions from realistic mixed-magma crystallizers and is based on the concept of a population balance of crystal particles along the particle size axis.¹⁷ The detailed development of the particle-number continuity equations and the moment transformation of the population balance may be found in Ref. 17.

A. Plug Flow Model

At steady state, with negligible breakage, the population balance is given by¹⁷

$$\nabla \cdot \vec{V}_e n + \frac{\partial}{\partial L} (Gn) = 0 , \quad (1)$$

where n is the number population density of the system, and G is the linear growth rate, $\frac{dL}{dt}$. The internal coordinate is taken as the Stoke's diameter L , as determined by sedimentation techniques. The external coordinate system is represented by the single crystallizer length dimension, x . For small particles, and high velocities, V_x , the external linear velocity, may be taken as the plug flow velocity, u_x . Assuming that growth rate G remains independent of size, an

empirical observation known as McCabe's ΔL law, which often holds true, then Eq. (1) reduces to

$$u_x \frac{\partial n}{\partial x} + G \frac{\partial n}{\partial L} = 0 \quad . \quad (2)$$

Equation (2) is the plug flow equation that includes the following assumptions:

- Steady state is achieved
- Linear velocity = plug flow velocity = constant
- Negligible breakage is achieved
- Growth rate is independent of size.

Multiplying Eq. (2) by $L^j dL$, and integrating from zero to infinity, we have

$$\int_0^\infty L^j u_x \frac{\partial n}{\partial x} dL + \int_0^\infty L^j G \frac{\partial n}{\partial L} dL = 0 \quad , \quad (3)$$

or

$$u_x \frac{\partial}{\partial x} \int_0^\infty L^j n dL + G \int_0^\infty L^j dn = 0 \quad . \quad (4)$$

Taking the second integral by parts, we have

$$u_x \frac{\partial}{\partial x} \int_0^\infty L^j n dL + G \left(L^j n \Big|_0^\infty - j \int_0^\infty L^{j-1} n dL \right) = 0 \quad . \quad (5)$$

Let us introduce the j th moment of the population defined by the integral, $m_j = \int_0^\infty L^j n \, dL$. If N is the total number of particles, the initial population density is $n_x^0 = (dN/dL)_{L \rightarrow 0}$ and the nucleation rate is $B_x^0 = (dN/dt)_{L \rightarrow 0}$. The boundary conditions are $n_x^0 = B_x^0/G_x$ and $n_y^0 = 0$. Here, the notation $r_x^L = r(x, L)$ is used. Equation (5) becomes

$$u_x \frac{dm_j}{dx} + (0)^j B^0 - j G m_{j-1} = 0 \quad (6)$$

where $j = 0, 1, 2, \dots$, and $(0)^j = 0$ when $j \neq 0$ and $(0)^0 = 1$ when $j = 0$.

The equations given by Eq. (6) are the moment equations for the plug flow model.

We will now introduce the retention time, τ , defined by $\tau = \bar{x}/u_x$, where \bar{x} is the effective length of the plug flow reactor in cm, and u_x is the plug flow velocity in cm^3/s . For an ideal plug flow reactor, each infinitesimal reactant volume will have the same retention time.² The quantities C_0 , the initial concentration ($x = 0$), and C_s , the concentration of the saturated solution, will also be used.

It will be more convenient to use dimensionless quantities in the discussion. The new quantities will be normalized in terms of the initial conditions where $x = 0$. The dimensionless external coordinate becomes $z = x/\bar{x}$, the dimensionless internal coordinate becomes $\xi = L/G_0 \tau$, and the dimensionless population density becomes $y = n/n_0^0$ where $n_0^0 = B_0^0/G_0$. The dimensionless concentration becomes $\beta = C/C_0$ and the dimensionless saturated concentration becomes $\beta_s = C_s/C_0$.

The dimensionless moments of the population, f , are

$$f_j = \int_0^\infty \xi^j y \, d\xi = \frac{m_j}{B_0^0 (G_0 \tau)^j \tau} . \quad (7)$$

The dimensionless plug flow moment equations are

$$f'_j - (0)^j \frac{B^0}{B_0^0} - j \frac{G}{G_0} f_{j-1} = 0 , \quad j=0, 1, 2, \dots \quad (8)$$

where $f'_j = df_j/dz$. The initial conditions are $f_j(0) = 0$, $j=0, 1, 2, \dots$.

The total solids concentration per unit volume of solids-free liquid is

$$M_T = \rho k_v m_3(x) = [C_0 - C(x)] \quad (9)$$

where ρ is the crystal density of PETN, 1.77 g/cm^3 , and K_v is the volume shape factor based on Stokes' law. In terms of the dimensionless quantities, Eq. (9) becomes

$$[1 - \beta(z)] = \frac{\rho K_v B_0^0 (G_0 \tau)^3 \tau}{C_0} f_3(z) . \quad (10)$$

At the exit of the reactor, $z = 1$. If the reaction is complete at $z = 1$, then $M_T / C_0 + \beta_s = 1$ and

$$\beta_s = \beta(1) . \quad (11)$$

This relationship is verified experimentally by weighing the product for a given volume of solids-free liquid. The experimental M_T results are given in Table 1. The table is an experimental verification of the completeness of reaction at $z = 1$.

TABLE I
EXPERIMENTAL M_T RESULTS

Sample	Measured M_T (g/cm ³)	C_0 (g/cm ³)	β_s	$M_T / C_0 + \beta_s$
3848	0.0008	0.0008	0.000	1.00
3849	0.0148	0.03	0.453	0.95
3851	0.0008	0.0008	0.000	1.00
3852	0.000775	0.0008	0.000	0.97
3853	0.00081	0.0008	0.000	1.01
3856	0.00144	0.00133	0.000	1.08
3857	0.00135	0.00133	0.000	1.01
3858	0.00134	0.00133	0.000	1.01
3861	0.00177	0.002	0.1125	0.99
3862	0.00171	0.002	0.1125	0.97
3863	0.00169	0.002	0.1125	0.96
3864	0.00161	0.002	0.1125	0.92
3866	0.00114	0.001	0.000	1.14
3867	0.00114	0.001	0.000	1.14
3868	0.00114	0.001	0.000	1.14
3871	0.00205	0.002	0.1125	1.14
3872	0.00182	0.002	0.1125	1.02
3873	0.00177	0.002	0.1125	1.00
3874	0.00195	0.002	0.1125	1.09
3876	0.0218	0.0267	0.162	0.98
3877	0.0213	0.0267	0.162	0.96
3878	0.0221	0.0267	0.162	0.99
3881	0.0128	0.03	0.453	0.88
3882	a	0.03	0.453	a
3883	0.0154	0.03	0.453	0.97

^a M_T not measured because of filtering difficulties.

Using these results and substituting Eq. (11) into Eq. (10),

$$1 - \beta_s = \frac{\rho K_v B_0^0 (C_0 \tau)^3 \tau}{C_0} f_3(1) , \quad (12)$$

dividing Eq. (10) by Eq. (12) and rearranging,

$$\beta(z) = 1 + \frac{f_3(z)}{f_3(1)} \beta_s - \frac{f_3(z)}{f_3(1)} . \quad (13)$$

This is the relationship for the concentration as a function of the normalized external coordinate. The normalized external coordinate, z , will be referred to as the reaction coordinate.

For the case in which $\beta_s = 0$,

$$\beta(z) = 1 - \frac{f_3(z)}{f_3(1)} . \quad (14)$$

B. Dispersed Plug Flow Model

Consider the plug flow of a fluid, on top of which is superimposed some degree of intermixing, the magnitude of which is independent of position within the vessel. This is called the dispersed plug flow model.¹⁵

For molecular diffusion in the x -direction, the governing differential equation is given by Fick's law

$$u_x \frac{\partial n}{\partial x} + G \frac{\partial n}{\partial L} = D \frac{\partial^2 n}{\partial x^2} \quad (15)$$

where the parameter D , called the axial diffusion coefficient, uniquely characterizes the degree of backmixing between adjacent reactant

volume elements during flow. The dimensionless group $(D/u_x \bar{x})$, called the vessel dispersion number, is the parameter that measured the extent of axial dispersions. Thus

$\frac{D}{u_x \bar{x}} \rightarrow 0$ negligible dispersion, hence, plug flow,

$\frac{D}{u_x \bar{x}} \rightarrow \infty$ large dispersion, hence, mixed flow.

This model usually represents quite satisfactorily flow that deviates not too greatly from plug flow.¹⁵

Equation (15) may be rewritten as

$$-D \frac{\partial^2 n}{\partial x^2} + u_x \frac{\partial n}{\partial x} + G \frac{\partial n}{\partial L} = 0 . \quad (16)$$

Multiplying by $L^j dL$ and integrating from zero to infinity gives

$$\int_0^\infty \left(-D \frac{\partial^2 n}{\partial x^2} \right) L^j dL + \int_0^\infty \left(u_x \frac{\partial n}{\partial x} \right) L^j dL + \int_0^\infty \left(G \frac{\partial n}{\partial L} \right) L^j dL = 0 . \quad (17)$$

or

$$-D \frac{\partial^2}{\partial x^2} \left(\int_0^\infty n L^j dL \right) + u_x \frac{\partial}{\partial x} \left(\int_0^\infty n L^j dL \right) + G \int_0^\infty \frac{\partial n}{\partial L} L^j dL = 0 . \quad (18)$$

Defining the j th moment as before, $m_j = \int_0^\infty n L^j dL$, we have

$$-D \frac{d^2 m_j}{dx^2} + u_x \frac{dm_j}{dx} + G \int_0^\infty L^j dn = 0 . \quad (19)$$

Integrating by parts and evaluating $n = 0$ as $L \rightarrow \infty$ and $n = B^0/G$ as $L \rightarrow 0$

$$-D \frac{d^2 m_j}{dx^2} + u_x \frac{dm_j}{dx} - (0)^j B^0 - jGm_{j-1} = 0 . \quad (20)$$

Using the definitions given in Section C, namely,

$$\tau = \frac{\bar{x}}{u_x}, \quad z = \frac{x}{\bar{x}}, \quad \xi = \frac{L}{G_0 \tau}, \quad y = \frac{n G_0}{B_0^0}, \quad f_j = \frac{m_j}{B_0^0 (G_0 \tau)^j \tau},$$

we have

$$D \left(\frac{1}{\bar{x}^2} \right) \left(B_0^0 G_0^j \tau^{j+1} \right) \frac{d^2 f_j}{dz^2} - u_x \left(\frac{1}{\bar{x}} \right) \left(B_0^0 G_0^j \tau^{j+1} \right) \frac{df_j}{dz} + (0)^j B^0 + jG \left(B_0^0 G_0^{j-1} \tau^j \right) f_{j-1} = 0 . \quad (21)$$

Simplifying:

$$\frac{D}{u_x \bar{x}} \frac{d^2 f_j}{dz^2} - \frac{df_j}{dz} + (0)^j \frac{B^0}{B_0^0} + j \frac{G}{G_0} f_{j-1} = 0 . \quad (22)$$

Define the Péclet number, the reciprocal of the vessel dispersion number, $Pe = u_x \bar{x} / D$. The resulting dispersed plug flow moment equations are

$$\frac{1}{Pe} f_j'' - f_j' + (0)^j \frac{B^0}{B_0^0} + j \frac{G}{G_0} f_{j-1} = 0 \quad (23)$$

with the boundary conditions^{4,23} $f_j(0) - \frac{1}{Pe} f_j'(0) = 0$, and $f_j'(1) = 0$.

Equation 13 from Section A holds for the dispersed plug flow model, namely, $\beta(z) = 1 + \frac{f_3(z)}{f_3(1)} \beta_s - \frac{f_3(z)}{f_3(1)}$ and for $\beta_s = 0$, $\beta(z) = 1 - \frac{f_3(z)}{f_3(1)}$.

C. Kinetics

Equations (8) and (23) contain the quantities B^0/B_0^0 and G/G_0 , which represent the normalized nucleation and growth rate functions, respectively. In order to solve these equations, some kinetic assumptions must be made.

1. Nucleation. The initial nucleation rate, B_0^0 , is the rate of formation of nuclei at $z = 0$, the entrance of the reactor. The assumption is made that the initial nucleation rate is a function of the ratio R .

Equation (12) may be written in the form

$$B_0^0 = \left[\frac{1}{\rho K_v (G_0 \tau)^3 \tau f_s(1)} \right] C_0 (1 - \beta_s) = B_0^0(R) . \quad (24)$$

The total nucleation, B^0 , is assumed to be the product of the initial nucleation and a decay function of the form $(1 - z)^a$. The expression for B^0 is

$$B^0 = B_0^0(R)(1 - z)^a \quad (25)$$

and the nucleation ratio B^0/B_0^0 is

$$\frac{B^0}{B_0^0} = (1 - z)^a . \quad (26)$$

2. Growth. The initial growth rate at the entrance is G_0 . The initial growth rate is related to the mass-weighted mean particle size, \bar{L} , as follows:

\bar{L} , the mass-weighted mean particle size, is defined by the ratio of the 4th and 3rd moments ($L_{4,3}$ in Ref. 17)

$$\bar{L} = \frac{m_4(1)}{m_3(1)} , \quad (27)$$

and by Eq. (7),

$$\bar{L} = \frac{B_0^c (G_0 \tau)^4 \tau f_4(1)}{B_0^c (G_0 \tau)^3 \tau f_3(1)} = G_0 \tau \frac{f_4(1)}{f_3(1)} . \quad (28)$$

G_0 is assumed to be a function of the experimental parameter, R . The total growth rate, G , is assumed to be the product of the initial growth rate and decay function of the form $(1 - z)^b$, namely,

$$G = G_0(R)(1 - z)^b . \quad (29)$$

The growth ratio G/G_0 is

$$\frac{G}{G_0} = (1 - z)^b . \quad (30)$$

The moment equations, including the kinetic assumptions, are

$$\text{Plug Flow: } f_j^i - (0)^j (1 - z)^a - j(1 - z)^b f_{j-1}^i = 0 \quad (31)$$

$$\text{Dispersed Plug Flow: } \frac{1}{Pe} f_j^{ii} - f_j^i + (0)^j (1 - z)^a + j(1 - z)^b f_{j-1}^i = 0 . \quad (32)$$

Equations (31) and (32), together with the appropriate boundary conditions, can be solved numerically to obtain the j th moments of the

of the distribution. A discussion of the numerical methods can be found in Appendix A.

D. Inversion of the Moments

The solution of either the plug flow or dispersed plug flow moment equations by methods given in the Appendixes, gives a set of $\{f_j\}$ dimensionless moments. The number of moments used in this study is ten, that is, $j = 0, 1, \dots, 9$.

The set of moments can be approximated by the equation

$$f_j \approx \sum_{k=0}^9 \xi_k^j y_k \Delta \xi_k , \quad (33)$$

from which the dimensionless population distribution function, y_k , may be calculated for a given ξ_k and $\Delta \xi_k$ using matrix inversion techniques.

The cumulative weight fraction distribution is¹⁷

$$WW(L) = \frac{\rho_k v \int_0^L p^3 n(p) dp}{M_T} , \quad (34)$$

where $n(p)$ is the population density of particles having size less than L .

Substituting the value for M_T from Eq. (9), and cancelling $\rho_k v$,

$$WW(L) = \frac{\int_0^L p^3 n(p) dp}{\int_0^L L^3 n(L) dL} . \quad (35)$$

Substituting the dimensionless quantities given in Section V. A, namely, $n = n_0^0 y$ and $L = G_0 \tau \xi$, we have

$$WW(L) = \frac{\int_0^{\xi} p^3 y(p) dp}{f_3(1)} \quad (36)$$

where $y(p)$ is the dimensionless population density of particles having dimensionless size less than ξ .

Equation (36) may be approximated by the sum

$$WW(L) = \frac{1}{f_3(1)} \sum_{i=c}^{\xi} p_i^3 y_i(p) \Delta p_i , \quad (37)$$

that is, $WW(L_0) = \frac{1}{f_3(1)} (\xi_0^3 y_0 \Delta \xi_0)$, $WW(L_1) = \frac{1}{f_3(1)} (\xi_0^3 y_0 \Delta \xi_0 + \xi_1^3 y_1 \Delta \xi_1)$, $WW(L_2) = \frac{1}{f_3(1)} (\xi_0^3 y_0 \Delta \xi_0 + \xi_1^3 y_1 \Delta \xi_1 + \xi_2^3 y_2 \Delta \xi_2)$, etc.

E. Comparison of Theory with Experiment

The differential equations representing the dispersed plug flow model are solved for a given set of parameters a , b , and Pe . The resulting dimensionless moments are inverted to obtain the population distribution functions and finally, the cumulative weight fraction distribution is calculated by means of Eq. (37). This cumulative weight fraction distribution can be directly compared with experimentally determined distributions.

The moments of the population may be compared directly without inversion by converting cumulative weight fraction distribution data to

moments based on weight distribution, and then converting to moments based on a population distribution.

The weight distribution function is defined by¹⁷

$$W(L) = \frac{dWW(L)}{dL} \quad (38)$$

and the j th moment of the weight distribution function is

$$m_j(wt) = \int_0^\infty L^j W(L) dL \quad (39)$$

or, approximately,

$$m_j(wt) \approx \sum_i L_i^j \Delta [WW(L_i)] . \quad (40)$$

The weight distribution may be converted to population distribution by the equation¹⁷

$$W(L) = \frac{1}{m_3(\text{popl.})} L^3 n(L) , \quad (41)$$

from which the following relationships are derived:

$$m_j(wt) = \frac{m_{j+3}(\text{popl.})}{m_3(\text{popl.})} \quad (42)$$

and

$$m_j(wt) = (G_0 \tau)^j \frac{f_{j+3}}{f_3} \quad (43)$$

Equation (43) allows the comparison of experimental data with calculated quantities derived from the theoretical model directly, without moment inversion. An alternate method, which utilizes three of the moments, is the calculation of the coefficient of variation (C. V.) of the distribution. The coefficient of variation, or relative dispersion, is the measure of dispersion stated as a function of its average, that is,

$$C. V. = \frac{\sigma}{L} , \quad (44)$$

where σ is the standard deviation from the mean for the distribution.

The coefficient of variation may be calculated from the moments by

$$C. V. = \left(\frac{m_2(\text{wt})}{m_1^2(\text{wt})} - 1 \right)^{\frac{1}{2}} \quad (45)$$

and by

$$C. V. = \left(\frac{f_5 f_3}{f_4^2} - 1 \right)^{\frac{1}{2}} . \quad (46)$$

(Note that $m_0(\text{wt}) \equiv 1.$)

VI. EXPERIMENTAL

A. Apparatus

The crystallization apparatus consists of three sections: (1) the constant flow feed system, (2) the static mixer, and (3) the filtering system. A diagram of the apparatus is shown in Fig. 2.

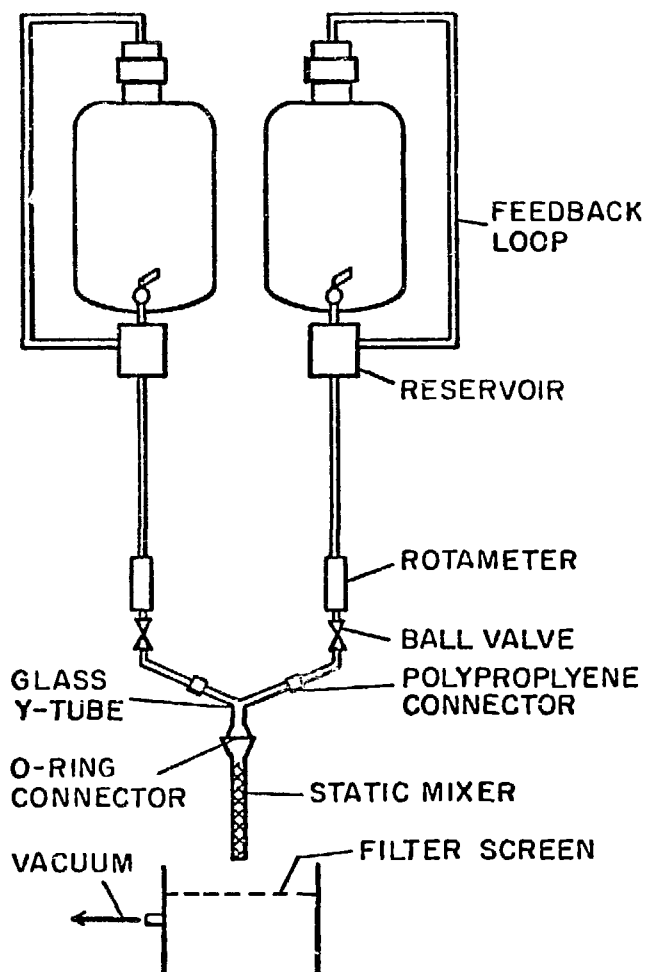


Figure 2.
PETN Crystallization Apparatus.

1. Constant Flow Feed System. There are two identical feed systems, one for the acetone-PETN solution, and one for the water. Each solution is held in a 24-liter capacity polyethylene bottle equipped with a polyethylene stopcock located through the sidewall at the bottom of the bottle. The solution is allowed to flow into a polyethylene reservoir (about 1 liter) situated just below the bottle and about 2 m above the static mixer. The polyethylene stopcock outlet extends into the reservoir. The liquid level is controlled in the reservoir by an airtight, 1.27-cm-o. d. polyethylene tube (feedback loop) that connects the top sidewall of the reservoir to the top of the bottle. If the liquid level in the reservoir drops below the tube inlet, the pressure above the liquid in the bottle increases to atmospheric allowing more liquid to pour into the reservoir. If the tube inlet is full of liquid, the feed solution will not flow into the reservoir. The solution is fed through a 1.27-cm-o. d. polyethylene tube to a rotameter ahead of the static mixer. The rotameters were calibrated using either pure acetone or water. Each solution is fed to the static mixer through a 0.635-cm-o. d. polyethylene tube.

The flow limitations of the system, including the rotameters, are:

Minimum acetone flow rate $1.3 \text{ cm}^3/\text{s}$

Maximum acetone flow rate $15.0 \text{ cm}^3/\text{s}$

Minimum water flow rate $1.0 \text{ cm}^3/\text{s}$

Maximum water flow rate 15.0 g/cm^3

2. Static Mixer. The effluent from the rotameters mix together at the first element of the static mixer by means of a glass Y-tube with a glass divider. The Y-tube is connected to the static mixer by means of an O-ring connector. Figure 3 is a schematic of the static mixer and Y-tube connector.

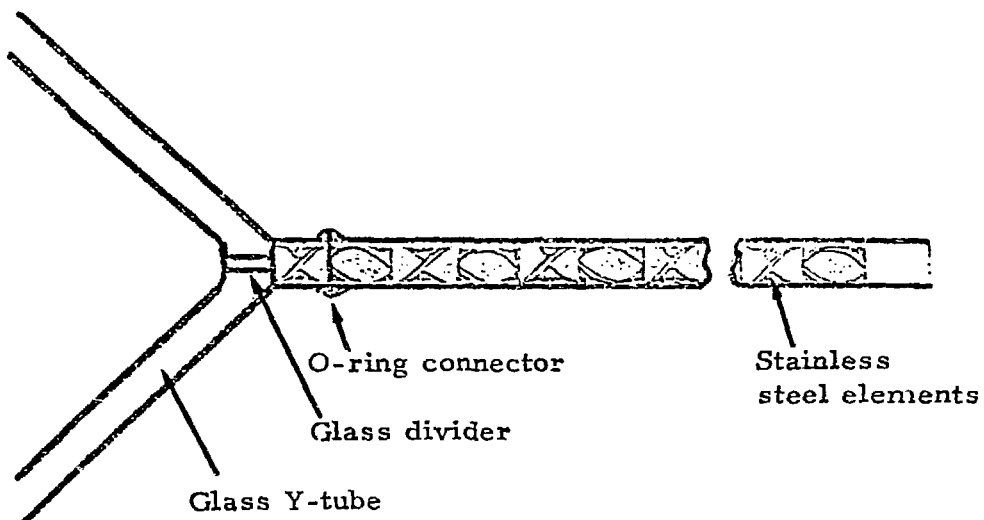


Figure 3.
Static Mixer.

The static mixer contains no moving parts. The mixing is achieved by the bow tie-shaped blades or elements. Their configuration imparts four basic motions to the flowing material:¹²

- Flow division--Each element divides material received from the preceding element.
- Flow reversal--The opposite twist of each succeeding element constantly reverses the circular direction of flow.

- Flow inversion--The material migrates from the center of the pipe to the outside walls and back.
- Backmixing--There is a constant change in flow profile. Velocity, pressure, and time have no influence upon the degree of mix. Pressure drop is low, and radial temperature differences are effectively eliminated.

Because of the continuous flow division reversal and flow inversion at every element of the mixer, ideal plug flow conditions are approached.²

The static mixer is a 0.635-cm-i.d. glass tube, 30.5 cm long, containing 24 stainless steel bow tie elements. The volume, as measured by water delivery at 20°C, is 9.0 cm³.

The holding time of the static mixer is calculated by the equation

$$\text{Holding time(s)} = \frac{\text{Volume of mixer (cm}^3\text{)}}{\text{Total volume flow rate (cm}^3/\text{s)}} . \quad (47)$$

Table 2 gives the scheme for holding times and flow rates used in the experiments.

Table 2
EXPERIMENT HOLDING TIMES AND FLOW RATES

<u>Acetone Solution Flow Rate (cm³/s)</u>	<u>Water Flow Rate (cm³/s)</u>	<u>R</u>
3.6	14.4	$\frac{1}{4}$
6.0	12.0	$\frac{1}{2}$
9.0	9.0	1
<u>Holding Time - 2.0 s</u> <u>Total Flow Rate - 4.5 cm³/s</u>		
1.13 ^a	3.38	$\frac{1}{3}$
2.25	2.25	1
3.0	1.5	2
3.38	1.13	3

^aThis is below the rotameter measurement limit. The flow rate was measured with a graduate and stopwatch.

3. Filtering System. Small samples (about 2 g) were collected on a 350-cm³ tared Buchner funnel with a fritted glass disc (medium porosity) mounted on a 2-liter suction flask. The volume of the solids-free liquid collected in the flask was measured. The PETN sample was washed with distilled water and dried under vacuum for 18 h at 65°C. The dried sample was weighed on a single-pan analytical balance. The data were used to calculate the M_T value for the run.

Large samples (30 to 50 g) were collected on a 29-cm-diam stain-
less steel screen nominally rated at 5 μ m. The screen was mounted
on a holder that was on a stainless steel can (about 10-liter capacity)
equipped with a vacuum connection.

B. Materials

- PETN--The PETN used was recrystallized Cap Grade (Lot 4-28-32) purchased from Du Pont. The material was analyzed for Group WX-3 use. The result of the nitrogen analysis is 17.26% N. The theoretical value is 17.72% N.
- Acetone--The acetone used was Analytical Reagent Grade.
- Water--Distilled water was used.
- Static Mixer--A Kenics Static Mixer,* purchased from Kenic's Corporation, Danvers, MA, was used.
- Metal Filter Screen--A furnace-sintered woven wire mesh filter screen nominally rated at 5 μ m was purchased from Pall Trinity Micro Corporation, Cortland, NY. A type 304 stainless steel filter screen, nominally rated at 5 μ m, was purchased from The Bendix Corporation, Filter Division, Madison Heights, MI.
- Plastic Fittings--All connections exposed to the acetone-PETN solution were made from polypropylene tube fittings purchased from United States Plastic Corporation, Lima, OH.

*Registered trademark.

C. Procedure

The acetone-PETN solution (about 10 liters) was adjusted to $20 \pm 3^\circ\text{C}$ and placed into the polyethylene bottle. The PETN concentration was 0.5 wt% for $R \leq 1$, and 5.0 wt% for $R > 1$. The distilled water (about 20 liters) was adjusted to $20 \pm 3^\circ\text{C}$ and placed in the second polyethylene bottle. The solutions were allowed to flow into their respective reservoirs and the bottles and feedback loops were checked for air leaks. The control valves were adjusted for the proper R-value to be used. The total flow rate was checked with a stopwatch and graduate. After allowing at least 30 s for equilibration, the metal screen was placed into position for collection of the sample. During the run, the rotameters were monitored for proper flow. Usually no further adjustment was necessary unless precipitated PETN began plugging the mixer. Precipitate buildup was significant for $R > 1$ runs. If precipitate buildup did occur, the sample collection was stopped and the mixer was "cleared" by opening the acetone solution to maximum flow until the precipitate redissolved in the acetone. After clearing the mixer, the flow was readjusted and the sample collection began again. During the run, the small sample was collected in a Buchner funnel with a fritted glass disc for M_T measurements. The procedures for each R value are summarized below:

$R = \frac{1}{4}$ (Batches 3848, 3851, * 3852, and 3853)

The acetone-PETN feed solution consisted of 39.75 g of PETN in 10 liters of acetone (0.5 wt%). The acetone-PETN flow rate was 3.6 cm³/s, and that of the water was 14.4 cm³/s. The holding time for the reactor was 0.5 s. Some difficulties were encountered in filtering the product. There was a tendency for a slight buildup of liquid on the filter. This problem was circumvented by supplementing the metal filter with three additional 600-cm³ Buchner funnels with fritted glass discs that were used in rotation so that little or no fluid accumulation occurred. The precipitated PETN collected on the filters was combined to form a single batch.

$R = \frac{1}{3}$ (Batches 3866, 3867, and 3868)

The acetone-PETN flow rate was 1.13 cm³/s and that of the water was 3.37 cm³/s. The reactor holding time was 2.0 s. The feed solutions were similar to the $R = \frac{1}{4}$ runs. The same filtering procedure was used.

$R = \frac{1}{2}$ (Batches 3856, 3857, and 3858)

The acetone-PETN flow rate was 6.0 cm³/s and that of the water was 12.0 cm³/s. The reactor holding time was 0.5 s. The feed solutions were similar to the $R = \frac{1}{4}$ and $R = \frac{1}{3}$ runs. The filtering procedure was the same.

*Batch 3851 was found to be contaminated with a fibrous material originating from the acetone stock. The batch was not included in the study.

R = 1 (Batches 3861, 3862, 3863, 3864, 3871, 3872, 3873, and 3874)

Two reactor holding times were used. Batches 3861 through 3864 were made with an acetone-PETN solution flow rate of 9.0 cm³/s and water flow rate of 9.0 cm³/s, giving a holding time of 0.5 s. Batches 3871 through 3874 were made with an acetone-PETN solution flow rate of 2.25 cm³/s and water flow rate of 2.25 cm³/s, giving a holding time of 2.0 s. The feed solutions were similar to the R = $\frac{1}{4}$, R = $\frac{1}{3}$, and R = $\frac{1}{2}$ runs. No filtering difficulties were encountered, and there was no need to supplement the metal filter.

R = 2 (Batches 3876, 3877, and 3878)

The acetone-PETN feed solution consisted of 416.3 g of PETN in 10 liters of acetone (5.0 wt%). The PETN concentration was increased because of its large solubility in the combined acetone-water solvent. The acetone-PETN solution flow rate was 3.0 cm³/s and that of the water was 1.5 cm³/s. The reactor holding time was 2.0 s. A 0.5-s holding time was not used because of a rapid irreversible plugging that occurred at the higher flow rates. No filtering problems were encountered.

R = 3 (Batches 3881, 3882, and 3883)

The acetone-PETN feed concentration was 5.0 wt%. The acetone-PETN flow rate was 3.33 cm³/s and that of the water was 1.11 cm³/s. The reactor holding was 2.0 s. Higher flow rates were not used because of irreversible plugging in the mixer. Difficulties

with product filtering were encountered. It was necessary to supplement the 29-cm-diam metal filter with the three fritted glass filters and with an additional 29-cm-diam metal filter.

D. Particle Measurement

1. Photelometer Technique.^{7,13} The estimation of particle size distribution for subsieve particles below the 45- μm sieve size was made possible by a particle sedimentation-in-liquid method. In this method, a representative PETN sample is dispersed homogeneously in a 50-vol% mixture of n-octane and 1,1,2,2-tetrachloroethane in a sedimentation tube. The intensity of a collimated beam of light passed through the suspension is measured after varying sedimentation times, and at varying levels. The particle size distribution is calculated by means of Stoke's law.

About one gram of each PETN sample was placed in about 300 cm^3 of the dispersing medium. The slurry was stirred for about 30 min by means of an air-driven rotary stirrer. The suspension was examined microscopically at 60X magnification to ensure total deagglomeration. Duplicate photelometer runs were made.

The samples were wet sieved using PETN-saturated ethanol as the transfer fluid. The following sieve sizes were used: 250, 177, 125, 88, 62, and 45 μm . Photelometer results were used for sub 45- μm particles. Sieve analyses were used for the large particle size. The correlation of photelometer results with sieve analyses for HMX (octahydro-1,3,5,7-tetranitro-s-tetrazocine) is shown in Fig. 4.⁷

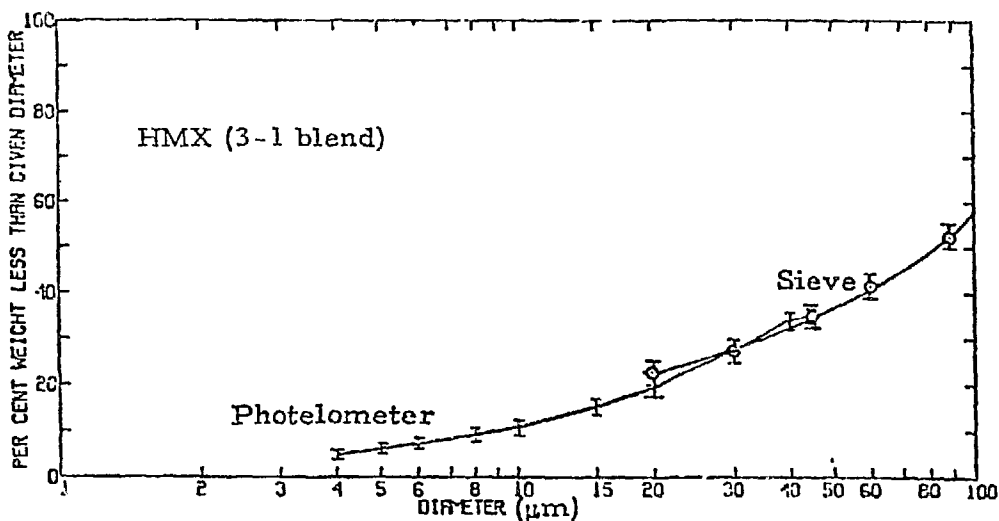


Figure 4.
Cumulative logarithmic plot of photelometer analysis of HMX and of sieve analysis of coarse fraction above 45 μm . Curve is average of four runs \pm one standard deviation.

2. Scanning Electron Microscopy. Each sample was photographed at 100, 300, and 1000X. The samples were gold shadowed to avoid any thermal effects on the heat-sensitive particles.

E. Detonator Test Firing

The PETN samples that were used in the detonators had the following pressed characteristics:

PETN pressed density 0.88 g/cm^3

PETN pressed diameter 4.064 mm

PETN pressed length 2.540 mm

PETN pressed mass 29 mg

1. Threshold Voltage Tests. Ten PETN pressings per sample were used. The PETN samples were initiated by a bursting gold

bridgewire 0.0381 mm diam and 1.016 mm long. The firing capacitance was 1 μ F per detonator. The firing cables consisted of a 4.41-m-long cable (21-C-31) connected to a 0.457-m-long cable (31-L-121) by means of a double-ended connector. The inductance of the cables plus bridgewire was 1.0413 μ H and the resistance was 0.266 Ω . The Bruceton "up and down" method⁶ of determining the 50% values of the firing voltages ($E_{0.5}$) was used.

2. Transit Time Tests. Two detonators per sample were fired.

A high density (1.65 g/cm³) PETN pressing 7.62 mm diam by 1.143 mm long was added to the PETN sample to increase the output light intensity. The transit time contribution of the high density PETN is a known constant for the tests. Any resulting variations in t_m are due to the PETN samples. The measured t_m value is the difference in time of the appearance of light between the bursting bridgewire and the shock wave breakout. The light appearances are observed with a rotating mirror camera (RMC).

The bridgewire used in the t_m tests is the same type as that used in the $E_{0.5}$ measurements. The firing capacitance was 1 μ F with a firing voltage of 2500 V per detonator. The firing cables used consisted of a 1.524-m-long cable (21-C-31) connected to a 0.762-m-long cable (31-L-121) by means of a double-ended connector. The

inductance of the cables plus bridgewire was $0.5389 \mu\text{H}$ and the resistance was 0.191Ω .

VII. RESULTS

A. Experimental Particle Size Distributions

The cumulative weight distribution curves for all R-values are shown in Figs. 5a through 5f. The error bars represent standard deviations. Photelometer runs were sufficient for $R < 1$; for $R \geq 1$, the photelometer method was supplemented by sieves. Table 3 summarizes the particle size characteristics of the products.

Table 3
PARTICLE SIZE CHARACTERISTICS

<u>R-Value</u>	<u>Average \bar{L} (μm)</u>	<u>Average Coefficient of Variation</u>
$\frac{1}{4}$	12.2	0.34
$\frac{1}{3}$	12.7	0.35
$\frac{1}{2}$	13.3	0.40
1	30.2	0.49
2	41.0	0.47
3	63.5	0.52

Representative product scanning electron micrographs are shown in Figs. 6a through 6g.

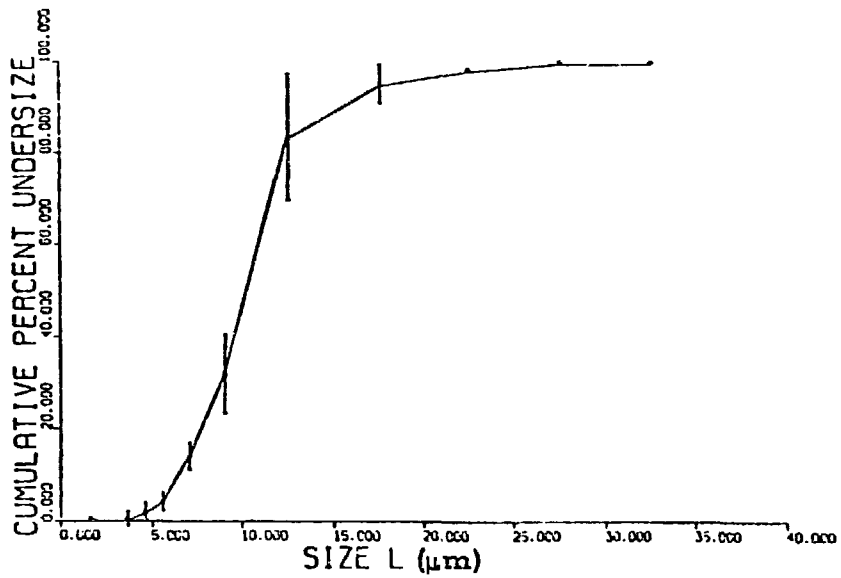


Figure 5a.
 $R = \frac{1}{4}$.

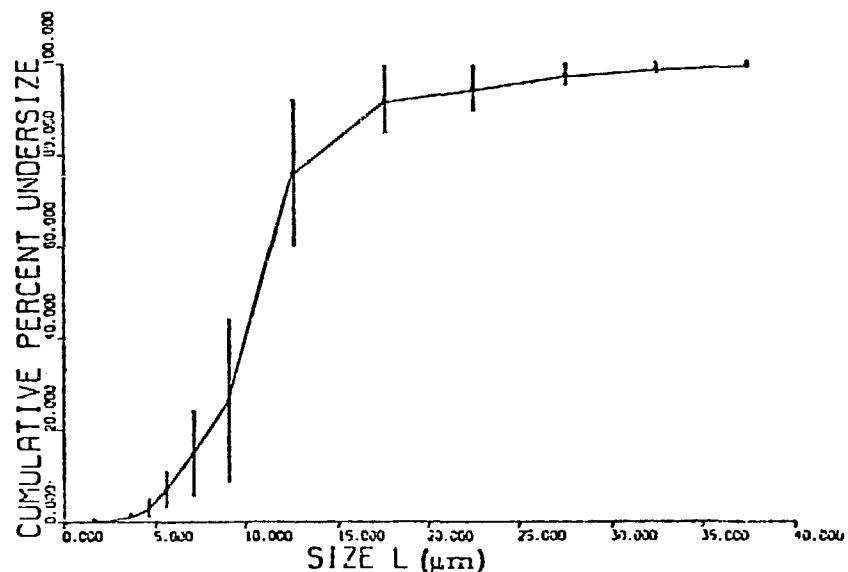


Figure 5b.
 $R = \frac{1}{3}$.

PETN Experimental Particle Size Distribution.

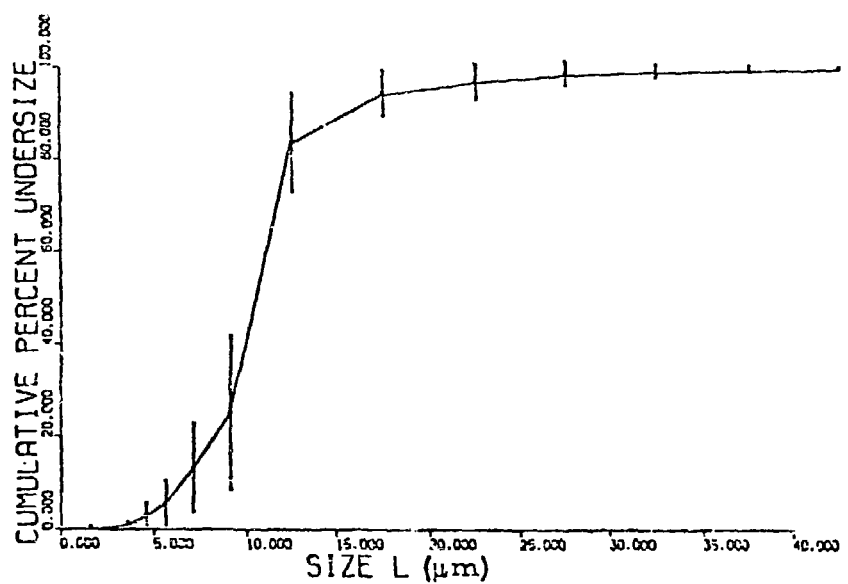


Figure 5c.
 $R = \frac{1}{2}$.

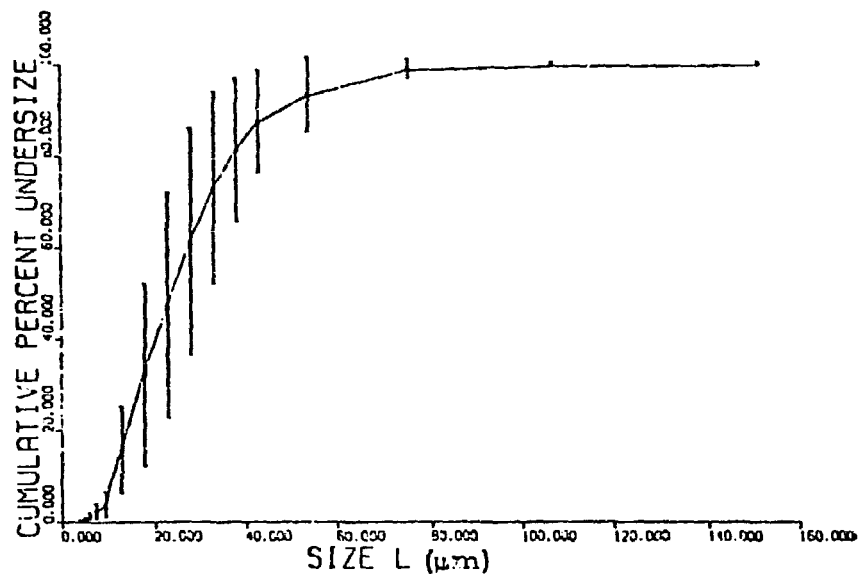


Figure 5d.
 $R = 1$.

PETN Experimental Particle Size Distribution.

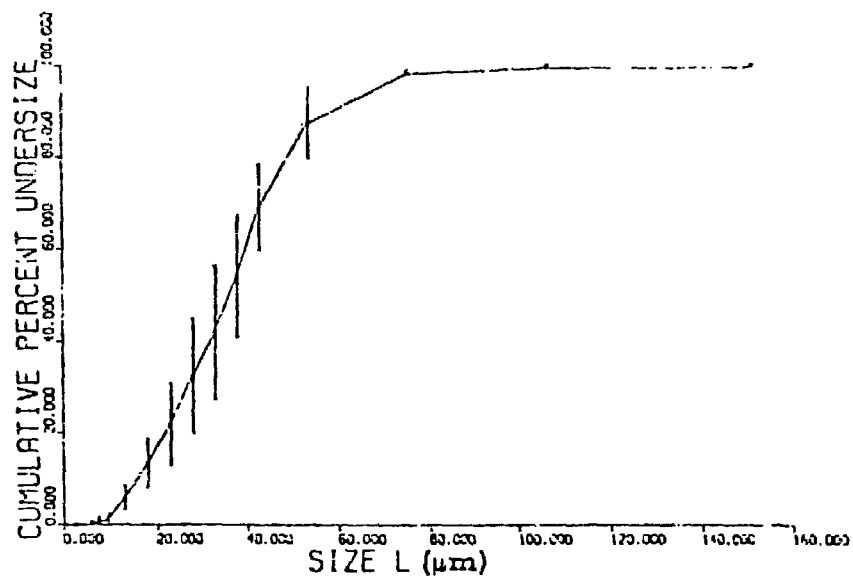


Figure 5e.
 $R = 2.$

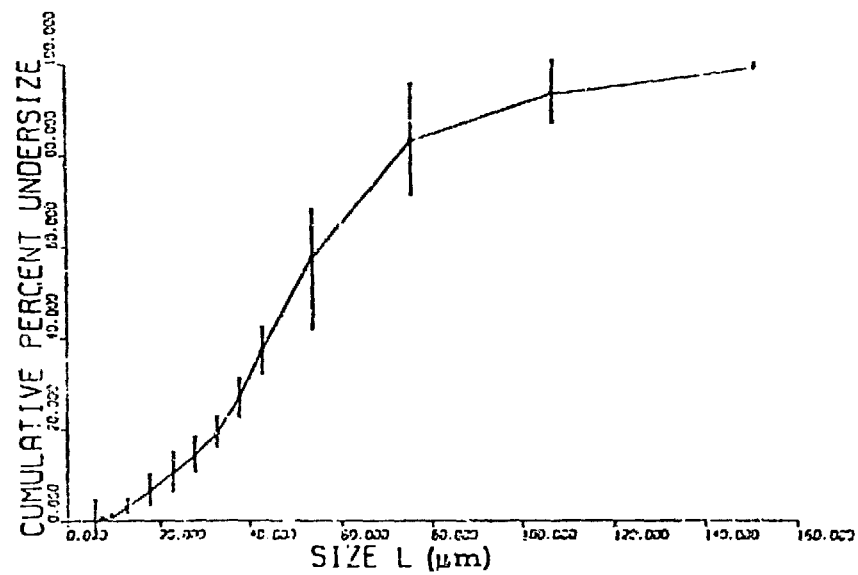
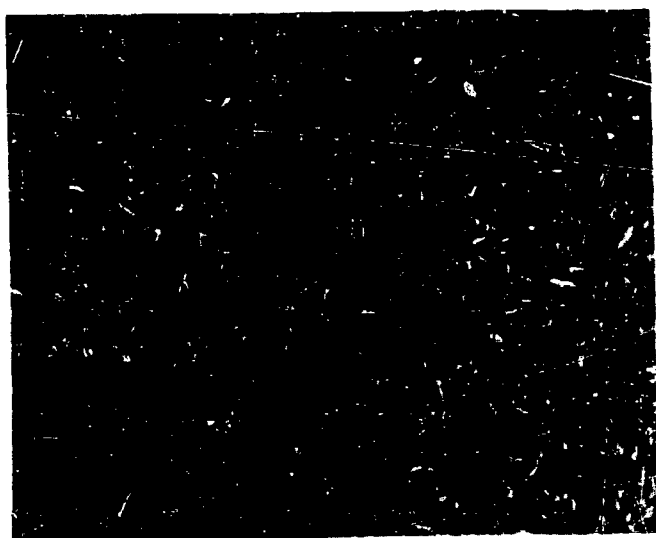


Figure 5f.
 $R = 3.$

PETN Experimental Particle Size Distribution.



100X



300X

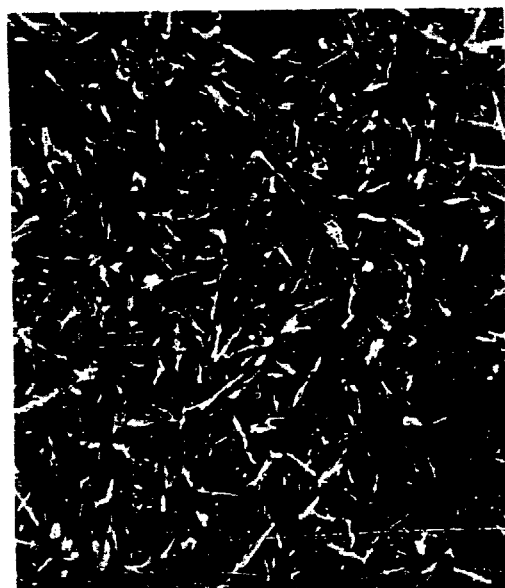


1000X

Figure 6a.
Scanning Electron Micrographs, PETN-3848 ($R = \frac{1}{4}$).



100X

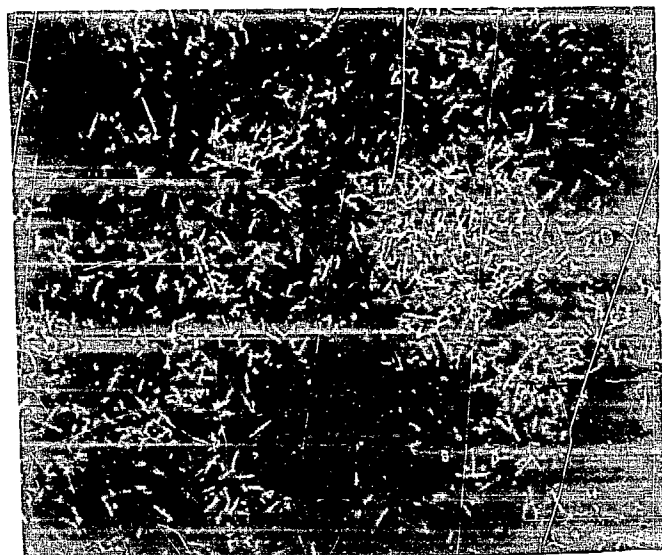


300X

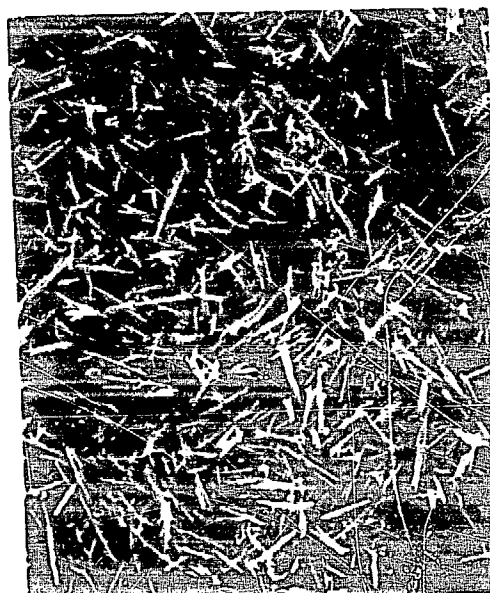


1000X

Figure 6b.
Scanning Electron Micrographs, PETN-3866 ($R = \frac{1}{3}$).



100X



300X

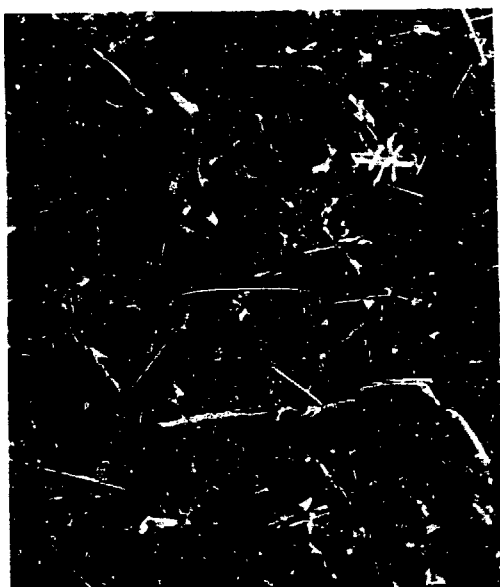


1000X

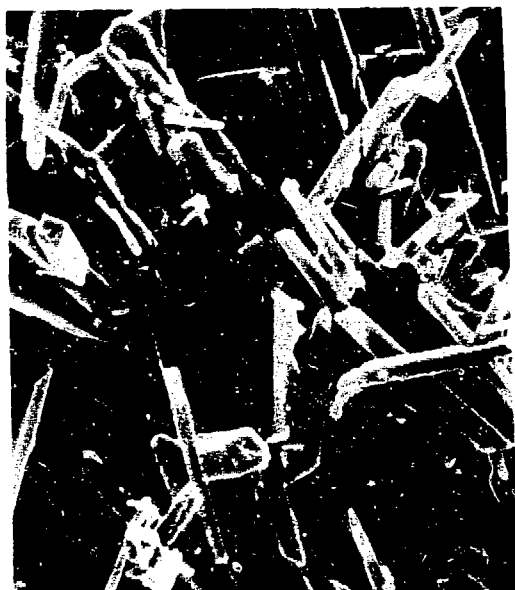
Figure 6c.
Scanning Electron Micrographs, PETN-3856 ($R = \frac{1}{2}$).



100X

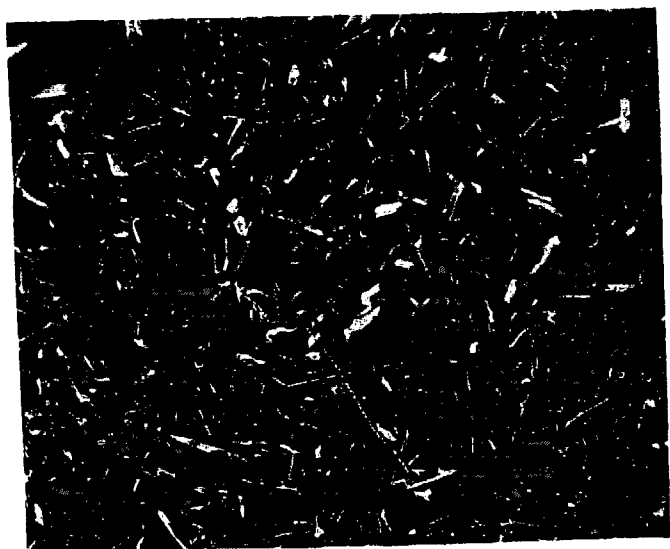


300X



1000X

Figure 6d.
Scanning Electron Micrographs, PETN-3861 ($R = 1$, $\tau = 0.5$ s).



100X



300X



1000X

Figure 6e.
Scanning Electron Micrographs, PETN-3871 ($R = 1$, $\tau = 2.0$ s).



100X



300X



1000X

Figure 6f.
Scanning Electron Micrographs, PETN-3877 (R = 2).



100X



300X



1000X

Figure 6g.
Scanning Electron Micrographs, PETN-3883 (R = 3).

B. Theoretical Model Predictions

1. Particle Size Distribution. The plug flow model calculations predict distributions that are significantly narrower than the experimentally determined ones. The coefficients of variation predicted by the plug flow model range from 0.11 to 0.21. The inclusion of the Péclet number causes the predicted distributions to broaden as Pe is lowered. The Péclet value of 250 gives results very nearly approaching plug flow values. The results described were obtained from the calculations based on the dispersed plug flow model.

A series of about 500 computer runs was made with combinations of the nucleation parameter, a , ranging from 1.0 to 4.0; the growth parameter, b , ranging from 0.5 to 1.7; and the diffusion parameter, Pe , ranging from 25 to 250. Additional runs were made to refine the calculations.

2. Effect of Varying Parameters. The effect of decreasing a (longer nucleation period) is primarily to increase the coefficient of variation. It also tends to decrease the mean particle size. It predicts a wider distribution of slightly smaller particles. The primary effect of increasing b (shorter growth period) is to decrease the mean particle size. It also increases the coefficient of variation. It predicts smaller particles having a wider distribution. The primary effect of decreasing Pe (increasing diffusion) is to increase the coefficient of variation with a small increase of particle size. The resulting best fit parameters are $a = 3.75 \pm 0.05$, $b = 1.56 \pm 0.02$, and $Pe = 51 \pm 1$. The resulting

predicted particle size distributions, compared with experimental results, are shown in Figs. 7a through 7f. Any further attempts to obtain a closer fit or to increase the coefficient of variation without deviation from a best fit gave unstable results. The resulting particle size distribution curves were not smooth, but rather the points were scattered in an oscillatory pattern.

3. Kinetics. A least-squares linear fit for \bar{L} vs R gives the equation, for \bar{L} in μm :

$$\bar{L} \approx (6.90 + 18.56R) \quad (48)$$

with a linear correlation factor of 0.99. From Eq. (28), we have

$$G_0 \tau = \frac{f_3(1)}{f_4(1)} \bar{L} . \quad (49)$$

For $a = 3.75$, $b = 1.56$, and $Pe = 51$, the ratio $[f_3(1)/f_4(1)]$ is 2.44.

For $G_0 \tau$ in μm , $G_0 \tau = 2.44 (6.90 + 18.56R)$ or

$$G_0 \tau = 16.84 + 45.29R . \quad (50)$$

Four experimental runs were made with $R = 1$ and a 0.5-s holding time. Four more runs were made with $R = 1$ and a 2.0-s holding time. The resulting particle size distributions, using the two holding times, were essentially the same. This information suggests that the true holding time of the system is either equal to, or less than 0.5 s.

$$\tau \leq 0.5 \text{ s} . \quad (51)$$

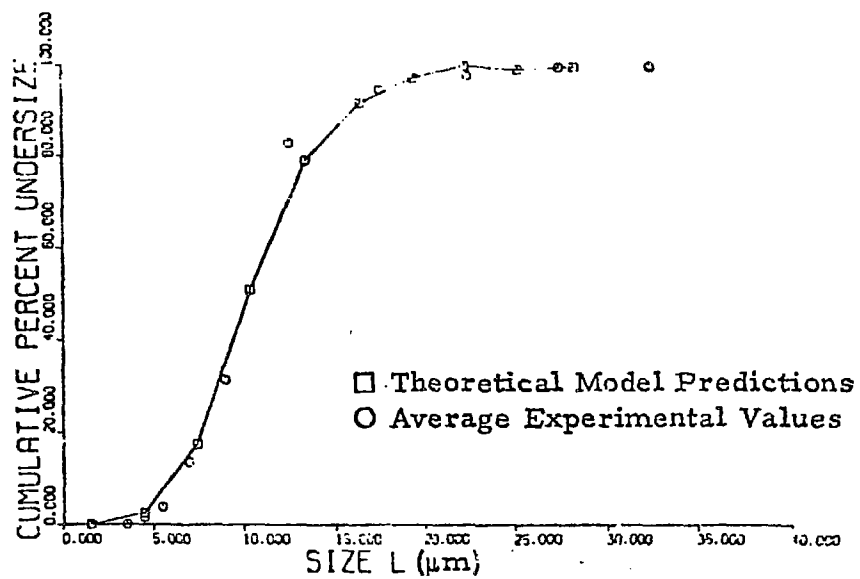


Figure 7a.

$$R = \frac{1}{4}.$$

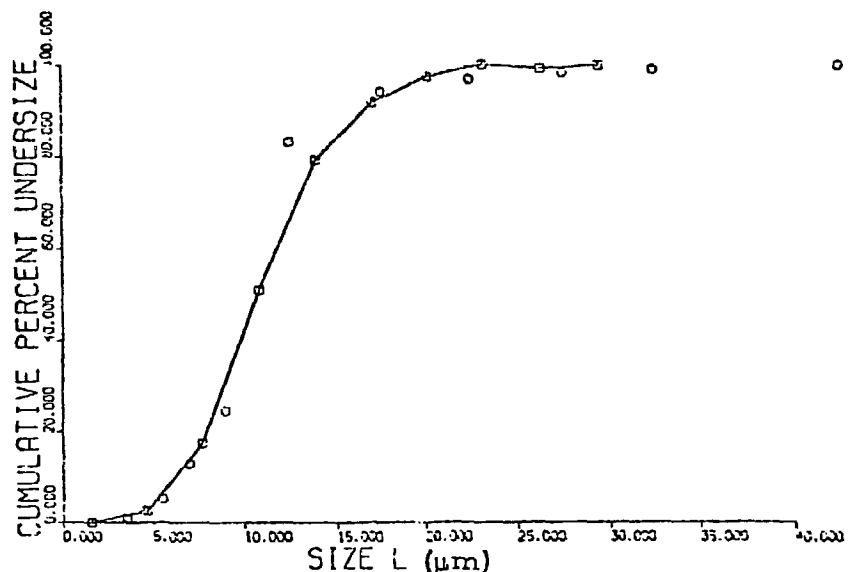


Figure 7b.

$$R = \frac{1}{3}.$$

Comparison of Theoretical Values with
Experimental Particle Size Distributions.

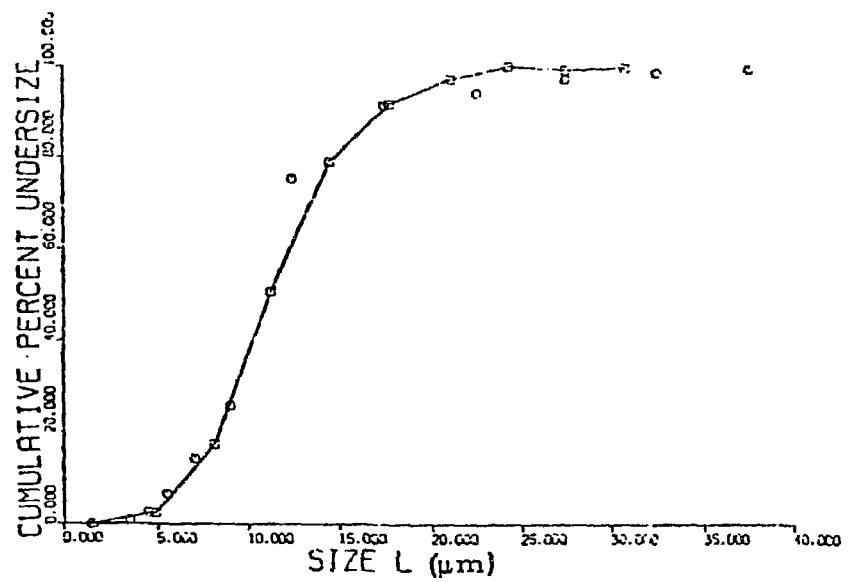


Figure 7c.
 $R = \frac{1}{2}$.

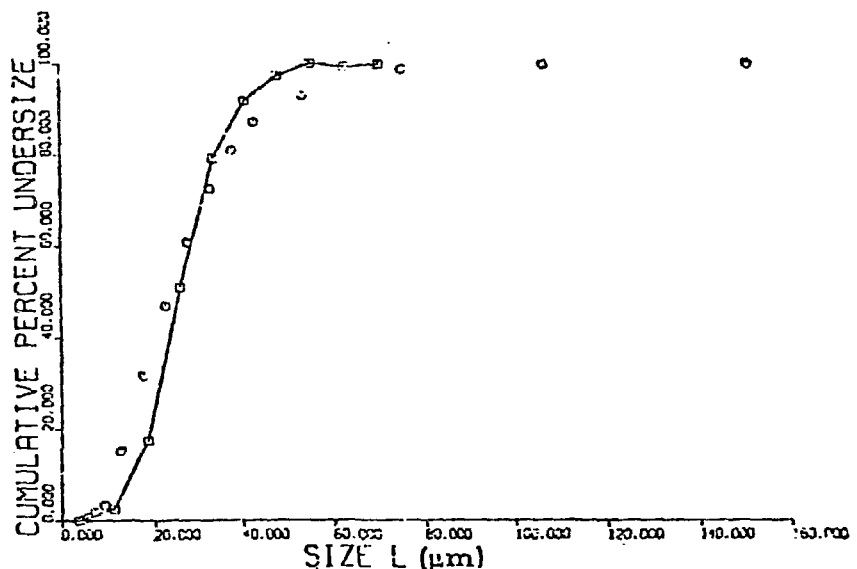


Figure 7d.
 $R = 1$.

Comparison of Theoretical Values with
 Experimental Particle Size Distributions.

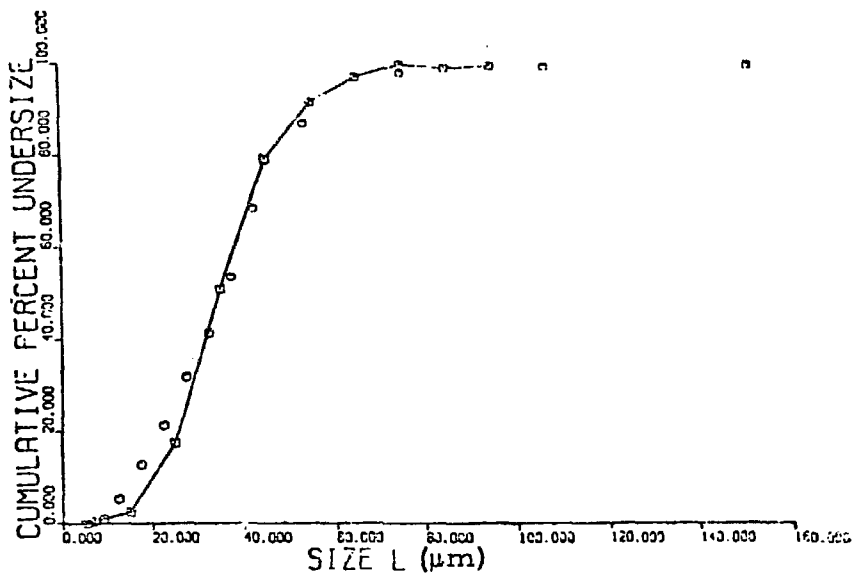


Figure 7e.
R = 2.

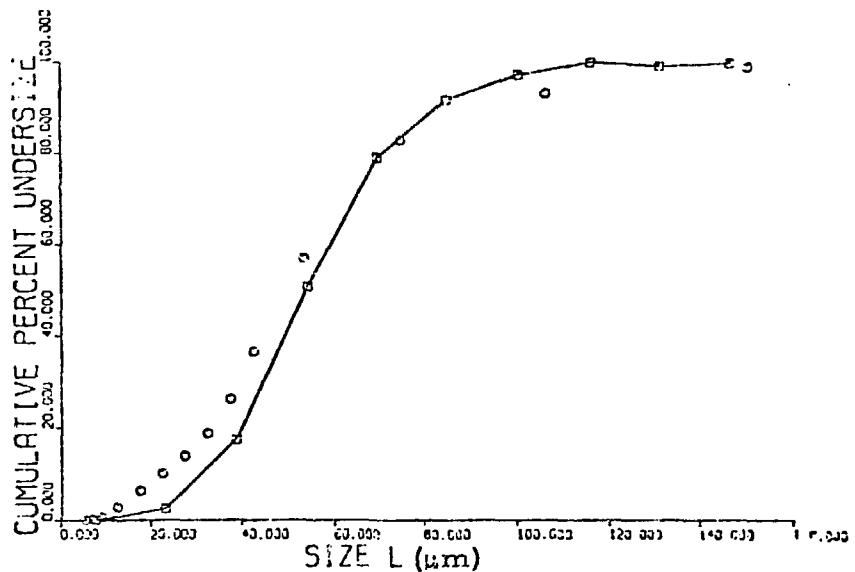


Figure 7f.
R = 3.

Comparison of Theoretical Values with
Experimental Particle Size Distributions.

If τ is taken equal to 0.5 s, the resulting calculations result in limiting quantities, subject to the flow rate range of the system used. The resulting kinetic quantities are limiting, or effective, kinetic quantities. These effective kinetics are valid for this system, but may not be valid if significantly higher flow rates are used, either by increasing the height of the column of solution above the static mixer, or by using a mechanical pump.

The effective initial growth rate in $\mu\text{m/s}$ is

$$G_0 = 33.68 + 90.58R \quad (52)$$

or

$$G_0 = 4.88E \quad . \quad (53)$$

The total effective growth rate kinetics are

$$G = (33.68 + 90.58R)(1 - z)^{1.56} \quad (54)$$

with G in $\mu\text{m/s}$. For purposes of simplicity, the quantity $B_0^0/C_0(1 - \beta_s)$ will be used in the discussion so that Eq. (24) becomes

$$\frac{B_0^0}{C_0(1 - \beta_s)} = \frac{1}{\rho K_v (G_0 \tau)^3 \tau f_3(1)} \quad (55)$$

where $\rho = 1.77 \text{ g/cm}^3$, $K_v = \pi/6$, $f_3(1) = 0.006745$ (using best fit parameters), $\tau = 0.5 \text{ s}$, and

$$\frac{B_0^0}{C_0(1 - \beta_s)} = \frac{K}{(G_0 \tau)^3} \quad (56)$$

where $K = [\rho K_v \tau f_3(1)]^{-1} = 320 \text{ cm}^3/\text{g} \cdot \text{s}$. Also,

$$\frac{B_0^0}{C_0(1 - \beta_s)} = \frac{K}{(16.84 + 45.29R)^3} \quad . \quad (57)$$

The total effective nucleation rate kinetics are

$$B^0 = 320 (16.84 + 45.29R)^{-3} C_0(1 - \beta_s)(1 - z)^{3.75} \quad (58)$$

with B^0 in nuclei/cm³·s.

Experimental values for G and B^0 are those in which the kinetic quantities were calculated from experimentally measured \bar{L} using Eqs. (49) and (56). These data, compared with those calculated directly from R by Eqs. (48), (50), and (57), are presented in Table 4.

Figure 8 is a plot of the normalized concentration of PETN in the acetone-water solvent, $\beta(z)$; the normalized growth rate, $G(z)$; and the normalized nucleation rate, $B^0(z)$; as functions of the reaction coordinate z . The early part of the reaction appears to be due to the combination of a rapidly decaying nucleation with a nearly linearly decaying growth. In the later part of the reaction, there is practically no nucleation, the growth rate being the primary mechanism at this stage.

The change of the growth rate as a function of concentration is shown in Fig. 9. The reaction proceeds from right to left along the concentration axis. The relationship is nearly linear, except for the initial and final stages of the reaction.

TABLE 4
CALCULATED KINETIC^a QUANTITIES

<u>R</u>	<u>L^b (experimental)</u>	Standard Deviation (μm)	<u>L (calculated)</u>	<u>Residual</u>	<u>Deviation (%)</u>	<u>Average Deviation (%)</u>
$\frac{1}{4}$	12.2	± 1.1	11.5	-0.7	6.1	
$\frac{1}{3}$	12.7	± 1.8	13.1	0.4	3.0	
$\frac{1}{2}$	13.3	± 2.3	16.2	2.9	17.9	8.9
1	30.2	± 9.0	25.5	-4.7	18.4	
2	41.0	± 5.2	44.0	3.0	6.8	
3	63.5	± 10.4	62.6	-0.9	1.4	

<u>R</u>	<u>G_0^c (experimental)</u>	<u>G_0 (calculated)</u>	<u>Residual</u>	<u>Deviation (%)</u>	<u>Average Deviation (%)</u>
$\frac{1}{4}$	59.54	56.33	-3.21	5.7	
$\frac{1}{3}$	61.98	63.87	1.89	3.0	
$\frac{1}{2}$	64.90	78.97	14.07	17.8	8.9
1	147.38	124.26	-23.12	18.6	
2	200.08	214.84	14.76	6.9	
3	309.88	305.42	-4.46	1.5	

<u>R</u>	<u>E_0^d (experimental)</u>	<u>E_0^d (calculated)</u>	<u>Residual</u>	<u>Deviation (%)</u>	<u>Average Deviation (%)</u>
$\frac{1}{4}$	0.97×10^7	1.14×10^7	0.17×10^7	14.9	
$\frac{1}{3}$	1.07×10^7	0.98×10^7	-0.09×10^7	9.2	
$\frac{1}{2}$	1.24×10^7	0.69×10^7	-0.55×10^7	79.7	28.6
1	1.42×10^6	2.36×10^6	0.94×10^6	39.8	
2	7.16×10^6	5.77×10^6	-1.39×10^6	24.1	
3	1.41×10^6	1.47×10^6	0.06×10^6	4.1	

^aEffective kinetic quantities.

^b L in μm .

^c G_0 in $\mu\text{m/s}$.

^d E_0^d in nuclei/ $\text{cm}^3 \cdot \text{s}$.

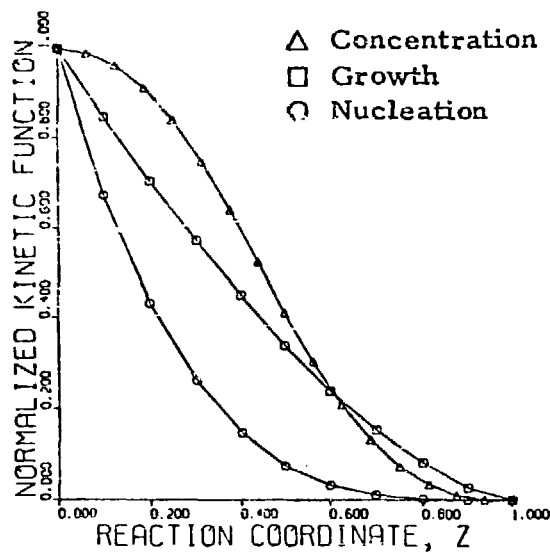


Figure 8.
Theoretical Kinetics Along Reaction Coordinate.

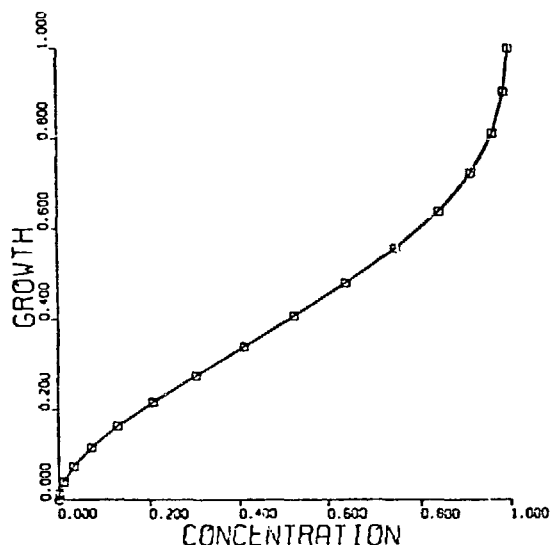


Figure 9.
Growth Rate Kinetics Along Reaction Coordinate.

The variation of the first four moments along the reaction coordinate is shown in Fig. 10. The 0th moment may be thought of as the total number of crystals in the volume under consideration. The rather large slope at the early part of the reaction may be due to the large nucleation occurring at this stage. The first moment represents the sum of the lengths of all the crystals in the distribution. This moment is controlled principally by growth. There appears to be an increase in the slope of the curve after the initial "surge" of nucleation. The second moment is related to the specific surface area and the third moment is related to the specific mass of crystals in the distribution.

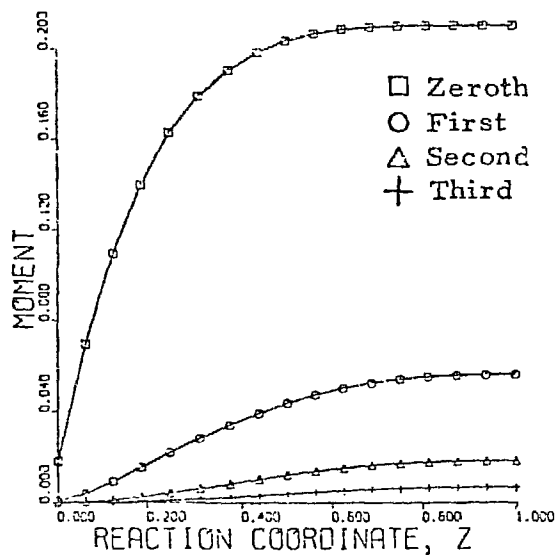


Figure 10.
Variation of Moments Along Reaction Coordinate.

C. Detonation Characteristics

The results of the threshold voltage measurements for the PETN samples are shown in Fig. 11. A polynomial regression was performed on the experimental data. The resulting second-degree polynomial curve is represented by the solid line in Fig. 11, and is referred to as the theoretical curve. The average percent deviation of the experimental data from the theoretical curve is 4.1. The experimental points are indicated in Fig. 11 by circles. Since the value for \bar{L} may be calculated from an R-value using Eq. (48), a correlation was made between $E_{0.5}$ and \bar{L} . The data are presented in Table 5. The equation for the calculation of $E_{0.5}$ from \bar{L} is

$$E_{0.5} = 1029.977 - 18.56256 \bar{L} + 0.19019 \bar{L}^2 \quad (59)$$

with \bar{L} in μm and $E_{0.5}$ in V.

The results of the transit time measurements for the PETN samples are shown in Fig. 12. The curve represented by the solid line resulted from a polynomial regression performed on the experimental data. The third-degree polynomial curve is referred to as the theoretical curve. The average percent deviation of the experimental data from the theoretical curve is 4.4. The correlation between t_m and \bar{L} is presented in Table 6. The equation for the calculation of t_m from \bar{L} is

$$t_m = 0.5562 + 0.03913 \bar{L} - 0.001227 \bar{L}^2 + 0.00001726 \bar{L}^3 \quad (60)$$

with \bar{L} in μm and t_m in μs .

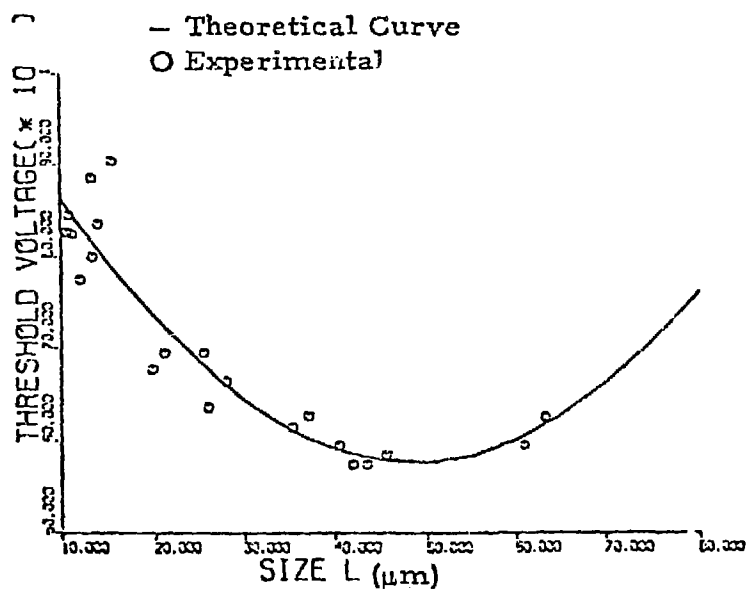


Figure 11.
PETN Detonator Threshold Voltages.

TABLE 5
CORRELATION OF THRESHOLD VOLTAGE WITH \bar{L}

\bar{L} (μm)	Average $E_{0.5}$ (V)	Standard Deviation (%)	Theoretical $E_{0.5}$ (V)	Deviation (%)
12.2	800	4.4	832	3.8
12.7	825	1.3	825	0.5
13.3	875	3.5	817	7.6
30.2	650	7.0	432	0.3
41.0	600	3.5	589	0.5
63.5	625	2.8	618	0.5

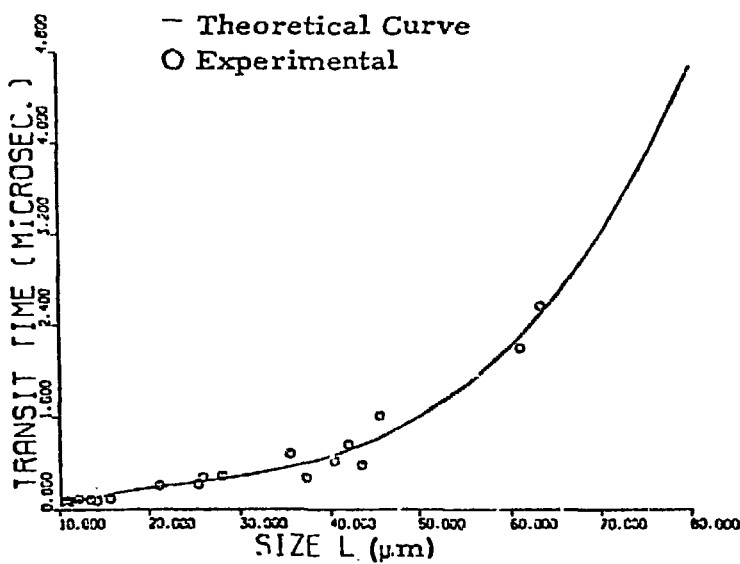


Figure 12.
PETN Detonator Transit Times.

TABLE 6
CORRELATION OF TRANSIT TIME WITH \bar{L}

\bar{L} (μm)	Average t_m (μs)	Standard Deviation (%)	Theoretical t_m (μs)	Deviation (%)
12.2	0.882	1.6	0.882	0.0
12.7	0.878	0.5	0.891	1.5
13.3	0.890	0.7	0.900	1.1
30.2	1.099	7.3	1.094	0.5
41.0	1.422	12.1	1.287	10.5
63.5	2.385	10.9	2.513	5.1

VIII. CONCLUSIONS

For a given R-value, the various quantities, including effective nucleation and growth rates, mass-weighted mean particle size, concentration function, transit time, and threshold voltage may be calculated using the equations summarized in Table 7.

The crystals obtained from the continuous plug flow crystallizer have narrow distributions and are fairly uniform in crystal habit. The dispersed plug flow model calculations provide a reasonably good prediction of these properties.

The objectives for developing a continuous reproducible recrystallization technique and a predictive model for the preparation of PETN have been achieved.

TABLE 7
SUMMARY OF THEORETICAL EQUATIONS

Quantity	Equation	Average Deviation from Experimental Results (%)
Mass-weighted mean particle size (μm)	$\bar{L} = 6.90 + 18.56 R$	8.9
Effective growth rate ($\mu\text{m/s}$)	$G(R, z) = (33.68 + 90.58 R)(1 - z)^{1.56}$	8.9
Effective nucleation rate (nuclei/ $\text{cm}^3 \cdot \text{s}$)	$B^0(R, z) = 320(16.84 + 45.29 R)^{-3} C_0 (1 - \beta_s)(1 - z)^{3.75}$	28.7
Concentration	$\beta(z) = 1 + \frac{f_3(z)}{f_3(1)} \beta_s - \frac{f_3(z)}{f_3(1)}$	a
Threshold voltage (V)	$E_{0.5} = 1029.977 - 18.56256 \bar{L} + 0.19019 \bar{L}^2$	4.1
Transit time (μs)	$t_m = 0.5562 + 0.03913 \bar{L} - 0.001227 \bar{L}^2 + 0.00001726 \bar{L}^3$	4.4

^aNot determined.

APPENDIX A

NUMERICAL METHODS

The plug flow differential equation solutions were obtained by means of a Runge Kutta method. The IBM System/360 Scientific Subroutine Package, DRKG, was used. The IBM System/360 Scientific Subroutine Package, SIMQ, was used to obtain the solutions of the simultaneous linear equations. The runs were made on an IBM-360 Model 50 computer. Brief descriptions of DRKG and SIMQ are given below.

DRKG FROM THE SCIENTIFIC SUBROUTINE PACKAGE

SUBROUTINE DRKGS

PURPOSE

TO SOLVE A SYSTEM OF FIRST ORDER ORDINARY DIFFERENTIAL EQUATIONS WITH GIVEN INITIAL VALUES.

USAGE

CALL DRKGS (PRMT, Y, DERY, NDIM, IHLF, FCT, OUTP, AUX)
PARAMETERS FCT AND OUTP REQUIRE AN EXTERNAL STATEMENT.

DESCRIPTION OF PARAMETERS

PRMT - DOUBLE PRECISION INPUT AND OUTPUT VECTOR WITH DIMENSION GREATER THAN OR EQUAL TO 5, WHICH SPECIFIES THE PARAMETERS OF THE INTERVAL AND OF ACCURACY AND WHICH SERVES FOR COMMUNICATION BETWEEN OUTPUT SUBROUTINE (FURNISHED BY THE USER) AND SUBROUTINE DRKGS. EXCEPT PRMT(5) THE COMPONENTS ARE NOT DESTROYED BY SUBROUTINE DRKGS AND THEY ARE

PRMT(1) - LOWER BOUND OF THE INTERVAL (INPUT),
PRMT(2) - UPPER BOUND OF THE INTERVAL (INPUT),
PRMT(3) - INITIAL INCREMENT OF THE INDEPENDENT VARIABLE (INPUT),
PRMT(4) - UPPER ERROR BOUND (INPUT). IF ABSOLUTE ERROR IS GREATER THAN PRMT(4), INCREMENT GETS HALVED. IF INCREMENT IS LESS THAN PRMT(3) AND ABSOLUTE ERROR LESS THAN PRMT(4)/50, INCREMENT GETS DOUBLED. THE USER MAY CHANGE PRMT(4) BY MEANS OF HIS OUTPUT SUBROUTINE.
PRMT(5) - NO INPUT PARAMETER. SUBROUTINE DRKGS INITIALIZES PRMT(5)=0. IF THE USER WANTS TO TERMINATE SUBROUTINE DRKGS AT ANY OUTPUT POINT, HE HAS TO CHANGE PRMT(5) TO NON-ZERO BY MEANS OF SUBROUTINE OUTP. FURTHER COMPONENTS OF VECTOR PRMT ARE FEASIBLE IF ITS DIMENSION IS DEFINED GREATER THAN 5. HOWEVER SUBROUTINE DRKGS DOES NOT REQUIRE AND CHANGE THEM. NEVERTHELESS THEY MAY BE USEFUL FOR HANDLING RESULT VALUES TO THE MAIN PROGRAM (CALLING DRKGS) WHICH ARE OBTAINED BY SPECIAL MANIPULATIONS WITH OUTPUT DATA IN SUBROUTINE OUTP.

Y - DOUBLE PRECISION INPUT VECTOR OF INITIAL VALUES (DESTROYED). LATER ON Y IS THE RESULTING VECTOR OF DEPENDENT VARIABLES COMPUTED AT INTERMEDIATE POINTS X.

DERY - DOUBLE PRECISION INPUT VECTOR OF ERROR WEIGHTS (DESTROYED). THE SUM OF ITS COMPONENTS MUST BE EQUAL TO 1. LATER ON DERY IS THE VECTOR OF DERIVATIVES, WHICH BELONG TO FUNCTION VALUES Y AT INTERMEDIATE POINTS X.
NDIM - AN INPUT VALUE, WHICH SPECIFIED THE NUMBER OF EQUATIONS IN THE SYSTEM.
IHLF - AN OUTPUT VALUE, WHICH SPECIFIED THE NUMBER OF BISECTIONS OF THE INITIAL INCREMENT. IF IHLF GETS GREATER THAN 10, SUBROUTINE DRKGS RETURNS WITH ERROR MESSAGE IHLF=11 INTO MAIN PROGRAM, ERROR PRMT(3)=0 OR IN CASE SIGN(PRMT(3)).NE.SIGN(PRMT(2))-MESSAGE IHLF=12 OR IHLF=13 APPEARS IN CASE PRMT(1)) RESPECTIVELY.
FCT - THE NAME OF AN EXTERNAL SUBROUTINE USED. THIS SUBROUTINE COMPUTES THE RIGHT HAND SIDES DERY OF THE SYSTEM TO GIVEN VALUES X AND Y. ITS PARAMETER LIST MUST BE X, Y, DERY. SUBROUTINE FCT SHOULD NOT DESTROY X AND Y.
OUTP - THE NAME OF AN EXTERNAL OUTPUT SUBROUTINE USED. ITS PARAMETER LIST MUST BE X, Y, DERY, IHLF, NDIM, PRMT. NONE OF THESE PARAMETERS (EXCEPT, IF NECESSARY, PRMT(4), PRMT(5),...) SHOULD BE CHANGED BY SUBROUTINE OUTP. IF PRMT(5) IS CHANGED TO NON-ZERO, SUBROUTINE DRKGS IS TERMINATED.
AUX DOUBLE PRECISION AUXILIARY STORAGE ARRAY WITH 8 ROWS AND NDIM COLUMNS.

REMARKS

THE PROCEDURE TERMINATES AND RETURNS TO CALLING PROGRAM, IF

- (1) MORE THAN 10 BISECTIONS OF THE INITIAL INCREMENT ARE NECESSARY TO GET SATISFACTORY ACCURACY (ERROR MESSAGE IHLF= 11),
- (2) INITIAL INCREMENT IS EQUAL TO 0 OR HAS WRONG SIGN (ERROR MESSAGES IHLF=12 OR IHLF=13,
- (3) THE WHOLE INTEGRATION INTERVAL IS WORKED THROUGH,
- (4) THE SUBROUTINE OUTP HAS CHANGED PRMT(5) TO NON-ZERO.

SUBROUTINES AND FUNCTION SUBPROGRAMS REQUIRED THE EXTERNAL SUBROUTINES FCT(X, Y, DERY) AND OUTP(X, Y, DERY, IHLF, NDIM, PRMT) MUST BE FURNISHED BY THE USER.

METHOD

EVALUATION IS DONE BY MEANS OF FOURTH ORDER RUNGE-KUTTA FORMULAE IN THE MODIFICATION DUE TO GILL. ACCURACY IS TESTED COMPARING THE RESULTS OF THE PROCEDURE WITH SINGLE AND DOUBLE INCREMENT.

SUBROUTINE DRKGS AUTOMATICALLY ADJUSTS THE INCREMENT DURING THE WHOLE COMPUTATION BY HALVING OR DOUBLING. IF MORE THAN 10 BISECTIONS OF THE INCREMENT ARE NECESSARY TO GET SATISFACTORY ACCURACY, THE SUBROUTINE RETURNS WITH ERROR MESSAGE IHLF=11 INTO MAIN PROGRAM.

TO GET FULL FLEXIBILITY IN OUTPUT, AN OUTPUT SUBROUTINE MUST BE FURNISHED BY THE USER.

FOR REFERENCE, SEE

RALSTON/WILF, MATHEMATICAL METHODS FOR DIGITAL COMPUTERS, WILEY, NEW YORK/LONDON, 1960, PF. 110-120.

SIMQ FROM THE SCIENTIFIC SUBROUTINE PACKAGE

SUBROUTINE SIMQ

PURPOSE

OBTAINT SOLUTION OF A SET OF SIMULTANEOUS LINEAR EQUATIONS,
 $AX = B$

USAGE

CALL SIMQ(A, B, N, KS)

DESCRIPTION OF PARAMETERS

A - MATRIX OF COEFFICIENTS STORED COLUMNWISE. THESE ARE DESTROYED IN THE COMPUTATION. THE SIZE OF MATRIX A IS N BY N.

B - VECTOR OF ORIGINAL CONSTANTS (LENGTH N). THESE ARE REPLACED BY FINAL SOLUTION VALUES, VECTOR X.

N - NUMBER OF EQUATIONS AND VARIABLES. N MUST BE .GT. ONE.

KS - OUTPUT DIGIT

0 FOR A NORMAL SOLUTION

1 FOR A SINGULAR SET OF EQUATIONS

REMARKS

MATRIX A MUST BE GENERAL.

IF MATRIX IS SINGULAR, SOLUTION VALUES ARE MEANINGLESS. AN ALTERNATIVE SOLUTION MAY BE OBTAINED BY USING MATRIX INVERSION (MINV) AND MATRIX PRODUCT (GMPRD).

SUBROUTINES AND FUNCTION SUBPROGRAMS REQUIRED

NONE

METHOD

METHOD OF SOLUTION IS BY ELIMINATION USING LARGEST PIVOTAL DIVISOR. EACH STAGE OF ELIMINATION CONSISTS OF INTER-CHANGING ROWS WHEN NECESSARY TO AVOID DIVISION BY ZERO OR SMALL ELEMENTS.

THE FORWARD SOLUTION TO OBTAIN VARIABLE N IS DONE IN N STAGES. THE BACK SOLUTION FOR THE OTHER VARIABLES IS CALCULATED BY SUCCESSIVE SUBSTITUTIONS. FINAL SOLUTION VALUES ARE DEVELOPED IN VECTOR B, WITH VARIABLE 1 IN B(1), VARIABLE 2 IN B(2), , VARIABLE N IN B(N).

IF NO PIVOT CAN BE FOUND EXCEEDING A TOLERANCE OF 0.0, THE MATRIX IS CONSIDERED SINGULAR AND KS IS SET TO 1. THIS TOLERANCE CAN BE MODIFIED BY REPLACING THE FIRST STATEMENT.

The dispersed plug flow differential equation solutions were obtained by means of finite difference techniques. The runs were made on a CDC-7600 computer. The complete program listings are given in Appendix C.

General discussions on Rung-Kutta methods, finite difference techniques, and solutions of simultaneous linear equations may be found in Refs. 8, 14, and 21.

APPENDIX B
DISPERSED PLUG FLOW MODEL LISTINGS

```

PROGRAM DRVR(OUT,FSET6=OUT)
DIMENSION H(100)
COMMON/EPSILON/EPS,EPS2
COMMON/VARY/NA,NB,NP
EPS=2.0**(-47)
EPS2=(2.0**(-48))*((1.0-2.0**(-48))
DO 100 NA=2,2
A=3.7+FLOAT(NA-1)*.05
DO 100 NB=2,2
D=1.54+FLOAT(NB-1)*.02
DO 100 NP=2,2
P=46.+FLOAT(NP-1)*5.
WRITE(6,2000)A,D,P
CALL PROG1 (B,N)
CALL PROG2 (B,N)
100 CONTINUE
2000 FORMAT(5X,4HA = ,F6.2,6H, B = ,F6.2,6H, P = ,F6.2)
STOP
END

      SUBROUTINE PROG1(B,NO)
C ** FINITE DIFFERENCE SOLUTION OF THE SECOND ORDER ODE
C     L(U) = -U#/P + U# = F  ON (ALEFT,ARIGHT)
C     B(U) = 0          DIRICHLET/NEUMANN/MIXED BC
      DIMENSION Q(16400), IT(4097), B(100)
      COMMON /DIFEQU/ ISIDEc,XSIDEc(10),P,NMOM,JDE
      COMMON /DMESH/ ALEFT,ARIGHT,H,N
      COMMON /APPROX/ U(10250),NH
      COMMON /OTHER/ MODE,MXITER,MXmesh
      PRINT 500
500  FORMAT(* PROBLEM*,15X,*BY FINITE DIFFERENCES*/)
C ** WRITE THE TITLE

      MODE = 1
      CALL SOLU(I,X,V)
C ** SET VARIOUS PARAMETERS FOR THE ODE
10    MODE = 2
      CALL SOLU(I,X,V)
C ** SOLVE THE JDE-TH EQUATION, FOR 0 ,LE. JDE ,LE. NMOM
      JDE = 1
      IJDE = 1
20    CONTINUE
C ** FROM THE FD EQUATIONS AND SIDE CONDITIONS,
C     GENERATE THE BANDED SYSTEM MATRIX IN Q AND THE RHS IN U
      MODE = 3
      CALL FDEAU(Q,U(IJDE))
C ** COMPUTE THE APPROXIMATE SOLUTION U BY BAND/RANSI
      CALL BAND(N,1,1,0,N,IT,DET)
      IF(ABS(DET) .LE. 1.E-7) PRINT 601,JDE,DET
601  FORMAT(2X,*++ FOR MOMENT EQUATION*,I4,* DET =,F14.7,* ++)
      CALL RANSI(N,1,1,0,N,IT,U(IJDE))
      IF(JDE .EQ. NMOM)          GO TO 30
      JDE = JDE + 1
      IJDE = IJDE + N
      GO TO 20
C ** THE SYSTEM IS SOLVED
C     OUTPUT THE MOMENTS U
30    CONTINUE
      IST = NMOM + 1
      IP = NMOM+1
      IST=0
      IST1=IST-1
      PRINT 501, (1,I=IST0,IST1)
501  FORMAT (* 1X *,10(* U*,I2,6X))
      IST=16
      DO 31  I=1,N,IST

```

```

      IOT=I-1
      PRINT 502, (IOT,(U(K),K=I,IP,N))
  31  IP = IP + IST
502 FORMAT(15,10E12.4)
      NQ = NMOM + 1
      DO 40 IFB = 1,NQ
      IFU = IFB*N
      B(IFB) = U(IFU)
40  CONTINUE
      END FD

```

```

      SUBROUTINE FDFOU(Q,U)
C  ** FILL SYSTEM MATRIX Q AND RHS U
      COMMON /DIFEGU/ ISIDEC,XSIDEC(10),P,NMOM,JDE
      COMMON /FDMFSH/ ALEFT,ARIGHT,H,N
      DIVERSION 0(1),U(1)
C  ** FIRST ZERO Q AND U , THEN FILL BY ROWS
      I2 = N
      I3 = I2 + N
      DO 1  I=1,N
          I2 = I2 + 1
          I3 = I3 + 1
          U(I) = P.
          Q(I) = P.
          Q(I2) = P.
1      U(I3) = P.
      HH = H*H
      ISIDEC = 1
      I = 1
      I2 = I + N
      I3 = I2 + N
      X = ALEFT
C  ** DO THE I-TH ROW
C  ** FIRST CHECK FOR SIDE CONDITIONS
      2 IF(X .EQ. XSIDFC(ISIDEC))      GO TO 3
C  ** THIS IS NOT A SIDE CONDITION ROW
      Q(I) = -1. - 0.5*P*H
      Q(I2) = 2.
      Q(I3) = -1. + 0.5*P*H
      CALL SOLU(I,X,V)
      U(I) = HH*V
      GO TO 4
C  ** THIS IS A SIDE CONDITION ROW
      3 J = I + (2 - ISIDEC)*N
      CALL FDSID(I,Q(J),U(I))
C  ** RETURN IF ALL ROWS FILLED
      4 IF(I .EQ. N)                  RETURN
C  ** UPDATE FOR NEXT ROW
      X = ALEFT + FLOAT(I)*H
      I = I + 1
      I2 = I2 + 1
      I3 = I3 + 1
      GO TO 2
      END FDEGU

```

```

      SUBROUTINE FDSTID(I,Q,U)
C ** FILL Q AND U AT THE SIDE CONDITION ROWS
COMMON /DIFEGU/ ISIDEC,XSIDFC(10),P,NHOM,JDE
COMMON /FDMFSH/ ALEFT,ARIGHT,M,N
DIMENSION Q(1)
HH = H*H
                           GO TO (10,20,99),I*IDEC
C ** MIXED BC  P*U(ALEFT) = U#(ALEFT) = U#(ARIGHT) = 0
10 X = XSIDFC(ISIDEC)
Q(1) = 1, + P*H
Q(N+1) = -1.
U = 0.
                           GO TO 90
20 X = XSIDEC(ISIDEC)
Q(1) = -2.
Q(N+1) = 2.
CALL SOLU(I,X,V)
U = HH*V
90 ISIDEC = ISIDEC + 1
                           RETURN
99
END FDSTID

      SUBROUTINE SOLU(IX,X,V)
COMMON /VAPY/ NA,NB,NP
COMMON /DIFEGU/ ISIDEC,XSIDEC(10),P,NHOM,JDE
COMMON /FDMFSH/ ALEFT,ARIGHT,M,N
COMMON /APPROX/ U(10250),NH
COMMON /OTHER/ MODE,MXITER,MXMESH
                           GO TO (10,20,30,40),MODE
C ** WRITE OUTPUT HEADING
10 CONTINUE
P=46.+FLOAT(P-1)*5.
NHOM = 9
NH = 64
DO 11 I=1,5
  IF(FLOAT(NH) .GE. P)          GO TO 12
11 NH = NH + 4
12 CONTINUE
NH = NH + P*H + NH + NH
PRINT 100, NHOM,P,NH
                           RETURN
100 FORMAT(44H -UJ##/P + UJ# = F1 + F2*UM , 0 ,LE, J ,LE.,I3,
      .      /* UJ(ALEFT) = UJ#(ALEFT)/P = 0 , UJ#(ARIGHT) = 0*/,
      .      /** P =*,E14.8,5X,*NH =*,IS//)
C ** INITIALIZE EVERYTHING
20 CONTINUE
ALEFT = 0.
ARIGHT = 1.
XSIDEC(1) = ALEFT
XSIDEC(2) = ARIGHT
H = (ARIGHT - ALEFT)/FLOAT(NH)
N = NH + 1
                           RETURN
C ** PROVIDE VALUE AT X OF RHS F1 + F2*U(J-1)
30 CONTINUE
V = F1(IX,X)
IF(JDE .EQ. V)          RETURN
I = (JDE - 1)*N + IX
V = V + F2(IX,X)*U(I)
                           RETURN
C ** PROVIDE VALUE AT X OF THE EXACT SOLUTION IF KNOWN
40 CONTINUE
V = VALUE
                           RETURN
END SOLU

```

```

FUNCTION F1(IX,X)
COMMON/VARY/NA,NB,NP
COMMON /DIFEGU/ ISIDEC,XSIDEC(10),P,NMOM,JDE
F1 = 0.
IF(JDE .NE. 0)                               RETURN
A=3.7+FLOAT(NA-1)*.05
F1 = P*(1. - X)**A
                                         RETURN
END F1

```

```

FUNCTION F2(IX,X)
COMMON/VARY/NA,NB,NP

COMMON /DIFEGU/ ISIDEC,XSIDEC(10),P,NMOM,JDE
F2 = 0.
IF(JDE .EQ. 0)                               RETURN
D=1.54+FLOAT(NB-1)*.02
F2=P*FLOAT(JDE)*(1.-X)**D
                                         RETURN
END F2

```

```

SUBROUTINE BAND(N,ML,MU,A,IA,INT,DET)
DIMENSION A(IA,1),INT(1)
DATA XND/0377777777777777/
IF(N,LT,1.OR,IA,LT,N,OR,ML,LT,0,OR,MU,LT,0) GO TO 12
IF(N,ED,1.OR,ML,ED,0) GO TO 9
MA = IA
LL = ML + MU + 1
NM = N - 1
DET = 1.
C ** SHIFT THE FIRST *ML* ROWS OF *A* TO THE LEFT
K = MU + 1
KJ = ML*MA
DO 3 I=1,ML
  IJ = I
  IL = I + KJ
  DO 1 J=1,K
    A(IJ) = -A(IL)
    IJ = IJ + MA
  1 IL = IL + MA
  K = K + 1
  DO 2 J=K,LL
    A(IJ) = 0.
  2 IJ = IJ + MA
  3 KJ = KJ + MA
C ** BEGIN GAUSS ELIMINATION LOOP
L = ML
KK = LL - 1
IL = KK*MA
DO 8 K=1,NM
  KP = K + 1
  IF(L,LT,N) L = L + 1

```

```

IF(KK.GT.N-K)  KK = N - K
C ** SEARCH FOR PIVOT ELEMENT IN COLUMN *K*
  I = X
  X = ABS(A(K))
  DO 4  J=KP,L
    IF(AHS(A(J)),LE,X)      GO TO 9
    I = J
    X = ABS(A(J))
4   CONTINUE
  INT(K) = I
  IF(I,EO,K)      GO TO 6
C ** INTERCHANGE ROWS OF *A* IF NECESSARY
  IJ = I
  KJ = K
  DO 5  J=1,LL
    X = A(KJ)
    A(KJ) = A(IJ)
    A(IJ) = X
    IJ = IJ + MA
5   KJ = KJ + MA
  DET = -DET
C ** BEGIN THE EXCHANGE STEP LOOP
  6  X = A(K)
    IF(X,FO,0.)      GO TO 11
    X = -1./X
    IK = K + MA
    KJ = K + IL
    DO 7  I=KP,L
      KJ = KJ + MA
      XX = A(I)*X
      A(KJ) = XX
      CALL ADDVEC(KK,XX,A(IK),MA,A(I+MA),MA,A(I),MA)
      A(I+IL) = 0.
7   CONTINUE
C ** END GAUSS ELIMINATION LOOP
  IF(A(N),EO,0.)      GO TO 11
  INT(N) = 0
  RETURN
C ** IN THIS CASE *A* IS UPPER TRIANGULAR
  9  DO 10  K=1,N
    IF(A(K),EO,0.)      GO TO 11
10   INT(K) = K
  DET = 1.
  INT(N) = 0
  RETURN
C ** MATRIX *A* MAY BE SINGULAR
11  DET = 0.
  INT(N) = K
  RETURN
C ** ERROR IN THE SYSTEM PARAMETERS *N*, *ML*, *MU*
12  DET = XND
  RETURN
END

```

```

SUBROUTINE RANS1(N,ML,MU,A,IA,INT,Y)
DIMENSION A(IA,1),INT(1),Y(1)
IF(L.EQ.1) GO TO 5
NM = N - 1
MA = IA
L = ML + MU
IF(ML.EQ.0) GO TO 3
LP = (L + 1)*MA
C ** BEGIN FORWARD SUBSTITUTION LOOP FOR COMPUTING THE SOLUTION *
KK = ML
DO 2 K=1,NM
  KP = K + 1
  IF(KK.GT.N-K) KK = N - K
  IF(INT(K).EQ.0) GO TO 1
C ** INTERCHANGE ROWS OF YY JUST AS WITH AA*
  J = INT(K)
  X = Y(K)
  Y(K) = Y(J)
  Y(J) = X
  1 CALL ADDVEC(KK,Y(K),A(K+LP),MA,Y(KP),1,Y(KP),1)
  2 CONTINUE
C ** BEGIN BACK SUBSTITUTION
  3 Y(N) = Y(N)/A(N)
  DO 4 I=1,N
    K = N - I
    KP = K + 1
    KK = L
    IF(KK.GT.I) KK = I
    Y(K) = (Y(K) - DOTPROD(KK,A(K+MA),MA,Y(KP),1))/A(K)
  4 CONTINUE
  RETURN
C ** MATRIX AA IS 1 BY 1
  5 Y(1) = Y(1)/A(1)
  RETURN
END

```

```

SUBROUTINE PHOG2 (B,N)
DIMENSION XI(100),DXI(100),A(100),B(100),X(100),TEMP(500),WW(100),
*XS1(100)
DO 3 J=1,N
  XI(J)=.05 + (FLOAT(J) - 1.)/10.
  XS1(J)=XI(J)
  3 DXI(J)=.1
  CALL FCT(A,XI,DXI,N)
  CALL UNSLIT(N,1,A,N,B,N,X,N,TEMP,DET,TEX,L)
  CALL OUTP(N,X,1)
  F3=1.0/B(4)
  DO 1 I=1,N
    1 XI(J)=XI(J)**3
    WW(1)=F3*XI(1)*DXI(1)*X(1)
    DO 2 J=2,N
      2 WW(J)=WW(J-1)+F3*XI(J)*DXI(J)*X(J)
  2005 FORMAT(5X,19HWEIGHT DISTRIBUTION)
  WRITE(6,2005)
  WRITE(6,2002)(WW(J),J=1,N)
  2002 FORMAT(10X,5E14.7)
  WRITE(6,2021)
  CALL PRNPLT(XS1,WW,1.,.,01,1,2,.025,0,0,N)
  2001 FORMAT(1H1)
  RETURN
END

```

```

SUBROUTINE FCT(A,XI,DXI,N)
DIMENSION A(N,1),XI(N),DXI(N)
DO 10 J=1,N
T=XI(J)
A(1,J)=DXI(J)
DO 10 I=2,N
10 A(I,J)=A(I-1,J)*T
RFTURN
END

```

```

SUBROUTINE OUTP(N,X,IX)
DIMENSION X(1)
NX=(N-1)*IX+1
WRITE(6,3000)(X(J),J=1,NX,IX)
3000 FORMAT(10X,5E14.7)
RETURN
END

```

```

SUBROUTINE UNSLIT(N,M,A,IA,B,IB,X,IX,SCR,DET,IEX,L)
C GIVES CORRECTLY ROUNDED SOLUTIONS OF A*X = B , WHERE A IS
C UNSYMMETRIC AND B IS N BY M , PROVIDED A IS NOT TOO
C ILL-CONDITIONED. USES PROCEDURES UNSDET, UNSACC, UNSSOL,
C INRPRO. COMPUTES THE DETERMINANT OF A IN THE FORM
C DET * 2**IEX . L IS THE NUMBER OF REFINEMENT STEPS.
C SCR IS WORKING STORAGE OF LENGTH AT LEAST N*(IA + L) + M*IB .
C THE PROCEDURE FAILS, AND PRINTS ERROR MESSAGES, IF THE LU
C FACTORIZATION OF A OR THE ITERATIVE REFINEMENT OF X FAILS.
10 FORMAT(1H0,37H MATRIX HAS ZERO ROW IN UNSDET AT STEP,14/)
11 FORMAT(1H0,43H MATRIX IS NEARLY SINGULAR IN UNSACC AT STEP,14/)
12 FORMAT(1H0,32H NO CONVERGENCE IN UNSACC AT STEP,14/)

DIMENSION A(IA,1),B(IB,1),X(IX,1),SCR(1)
C AA STARTS IN SCR(LA) , BB IN SCR(LB) , INT IN SCR(LI)
DO 1 J=1,N
  K = (J - 1)*IA
  DO 1 I=1,N
    L = K + I
1   SCR(L) = A(I,J)
LA = 1
LB = LA + IA*N
LI = LB + IB*M
C FORM LU FACTORS
CALL UNSDFT(N,SCR(LA),IA,DET,IEX,SCR(LI),SCR(LI),ILL)
IF(ILL.NE.0) GO TO 2
C ITERATIVE REFINEMENT
CALL UNSACC(N,M,A,SCR(LA),IA,B,SCR(LB),IB,X,IX,SCR(LI),L,ILL)
IF(ILL.EQ.0) RETURN
C ITERATIVE REFINEMENT FAILED
PRINT 12,ILL
RETURN
C LU FACTORIZATION FAILED
2 IF(ILL.GT.0) PRINT 11,ILL
ILL = -ILL
IF(ILL.GT.0) PRINT 10,ILL
RETURN
END

```

```

SUBROUTINE INRPRO(L,C1,C2,X,IX,Y,IY,D1,D2)
C ACCUMULATES THE SUM OF PRODUCTS X(K)*Y(K) AND ADDS IT
C TO THE INITIAL VALUE C1 + C2 IN DOUBLE PRECISION.
C D1 IS THE SINGLE PRECISION VALUE OF THE DOUBLE PRECISION
C SUM D. D2 IS THE SINGLE PRECISION DIFFERENCE D - D1.
C IF THE VECTOR LENGTH L IS NOT POSITIVE, THEN D = C1 + C2,
C SPEED OF EXECUTION OF THIS ROUTINE CAN BE GREATLY INCREASED
C BY HAND CODING. WHAT IS REQUIRED IS THAT THE SUMS AND
C MULTIPLICATIONS BE PERFORMED IN DOUBLE PRECISION.

```

```

DIMENSION X(1),Y(1)
DOUBLE PRECISION D,DX,DY
DX = C1
DY = C2
D = DX + DY
IF (L.LE.0) GO TO 2
I = 1
J = 1
DO 1 K=1,L
DX = X(J)
DY = Y(J)
D = D + DX*DY
I = I + 1X
J = J + 1Y
1 D1 = D
D2 = D - D1
RETURN
END

```

```

SUBROUTINE UNSQFT(N,A,IA,DET,IEX,INT,SCA,ILL)

```

```

C FORMS LU FACTORS OF A BY CRDIT METHOD WITH ROW EQUILIBRATION
C AND PARTIAL PIVOTING. OVERWRITES L AND U ON A, OMITTING
C UNITY DIAGONAL OF U, AND RECORDS ROW INTERCHANGES IN INT.
C COMPUTES THE DETERMINANT OF A IN THE FORM DET * 2**IEX.
C THE PROCEDURE FAILS IF A, AS MODIFIED BY ROUNDING ERRORS, IS
C SINGULAR OR NEARLY SINGULAR. USES PROCEDURE INRPRO. EPS IS
C THE (MACHINE-DEPENDENT) LEAST NUMBER X SO THAT 1. + X .GT. 1.
C DIMENSION A(IA,1),INT(13),SCA(1)
C DATA EPS /2.0**(-47)/
COMMON/FPSILON/EPS,EPS2
ILL = 0
C SCALE SO THAT SCA(J)*(A(I,)) HAS UNIT SUP NORM LENGTH
DO 2 I=1,N
X = 0.
DO 1 J=1,N
1 IF(ABS(A(I,J)).GT.X) X = ABS(A(I,J))
IF(X) 2,11,2
2 SCA(I) = 1./X
DET = 1.
IEX = 0
DO 10 K=1,N
C COMPUTE ENTRIES OF L IN COLUMN K
L = K
X = 0.
DO 3 J=K,N
CALL INRPRO(K-1,-A(I,K),0.,A(I,1),IA,A(1,K),1,Y,YY)
A(I,K) = -Y
Y = ABS(Y*SCA(I))
IF(Y.LT.X) GO TO 3
X = Y
L = I
3 CONTINUE
IF(L.EQ.K) GO TO 5
INTERCHANGE ROWS IF NECESSARY, SAVING INTERCHANGE INFORMATION
DET = -DET

```

```

      DO 4  J=1,N
      Y = A(K,J)
      A(K,J) = A(L,J)
      4  A(L,J) = Y
      SCA(L) = SCA(K)
      5  INT(X) = L
C     UPDATE DETERMINANT AND CHECK FOR NEARLY SINGULAR  A
      DET = DET*A(K,K)
      IF(X,LT,0.1HEPS)           GO TO 12
C     A IS OK THROUGH ROW K
C     SCALE DETERMINANT TO AVOID OVERFLOW
      6  IF(ABS(DET),LT,1.)       GO TO 7
      DET = DET*V,0625
      IEX = IEX + 4
      GO TO 6
      7  IF(ABS(DET),GE,2.0625)   GO TO 8
      DET = DET*16.0
      IEX = IEX - 4
      GO TO 7
C     COMPUTE ENTRIES OF  U  IN ROW K
      8  IF(K,EQ,N)              GO TO 10
      X = -1./A(K,K)
      KP = K + 1
      DO 9  J=KP,N
      CALL INRPRO(K=1,-A(K,J),0.,A(K,1),IA,A(1,J),1,Y,YY)
      9  A(K,J) = X*Y
      10 CONTINUE
      RETURN
C     A IS SINGULAR
      11 ILL = -1
      RETURN
C     A IS NEARLY SINGULAR
      12 ILL = K
      RETURN
      END

      SUBROUTINE UNSSOL(N,M,A,IA,B,IB,INT)
C     SOLVES  A*X = B  WHERE  A  IS UNSYMMETRIC AND  B  IS  N  BY  M.
C     MUST BE PRECFD BY PROCEDURE UNSDET TO PRODUC LU FACTORS
C     IN  A  WITH RECORD OF ROW INTERCHANGES IN  INT.  OVERWRITES
C     X  ON  B.  USES PROCEDURE  INRPRO.
C     DIMENSION A(IA,1),B(IB,1),INT(1)
C     INTERCHANGES OF  B
      DO 2  I=1,N
      IF(INT(I),EQ,1)           GO TO 2
      J = INT(I)
      DO 1  K=1,N
      X = B(I,K)
      B(I,K) = H(J,K)
      1  B(J,K) = X
      2  CONTINUE
      DO 5  K=1,N
      SOLVE 1AY = B
      DO 3  I=1,N
      CALL INRPRO(I=1,B(I,K),0.,A(I,1),IA,B(1,K),1,X,XX)
      3  B(I,K) = -X/A(I,I)
      SOLVE 0*X = Y
      B(N,K) = -B(N,K)
      DO 4  I=2,N
      I = N + 1 - IT
      CALL INRPRO(IT=1,B(I,K),0.,A(I,I+1),IA,B(I+1,K),1,X,XX)
      4  B(I,K) = -X
      5  CONTINUE
      RETURN
      END

```

```

      SUBROUTINE UNSAC(N,M,AA,IA,B,BH,TH,X,IX,INT,L,ILL)
C  SOLVES A*X = B WHERE A IS UNSYMMETRIC AND B IS N BY M,
C  USING PROCEDURE UNSSOL, MUST BE PRECEDED BY PROCEDURE UNSDET
C  TO PRODUCE LU FACTORS OF A IN AA WITH RECORD OF ROW
C  INTERCHANGES IN INT. COMPUTES RESIDUALS BB = B - A*X USING
C  PROCEDURE INRPRO, AND SOLVES A*D = BB, OVERWRITING D ON BB,
C  THEN OVERWRITES THE REFINEMENT X + D ON X. REPEATS THE
C  REFINEMENT SO LONG AS THE MAX CORRECTION AT ANY STEP IS LESS THAN
C  HALF THAT AT THE PREVIOUS STEP, UNTIL THE MAX CORRECTION IS LESS
C  THAN 2*EPS*(SUP NORM OF X). EXITS WITH ILL .NE. 0 IF THE
C  SOLUTION FAILS TO IMPROVE. L IS THE NUMBER OF ITERATIONS.
C  EPS IS THE (MACHINE-DEPENDENT) LEAST NUMBER T SUCH THAT
C  1. + T .GT. 1., AND EPS2 IS THE (MACHINE-DEPENDENT) GREATEST
C  NUMBER T SUCH THAT 1. + T .EQ. 1.
      DIMENSION AA(IA,1),AA(IA,1),B(IB,1),BB(IB,1),X(IX,1),INT(1)
C  DATA EPS /2.0**(-47)/ , EPS2 /(2.0**(-48))*(1.0 - 2.0**(-48))/,
COMMON/EPSILON/EPS,EPS2
      ILL = 0
C  SET UP FOR FIRST APPROXIMATE SOLUTION
      DO 1  J=1,M
        DO 1  I=1,N
          X(I,J) = 0.
1        BB(I,J) = B(I,J)
      L = 0
      D0 = 0.0

C  COMPUTE AND ADD THE CORRECTION
2  CALL UNSSOL(N,M,AA,IA,BB,IB,INT)
      L = L + 1
      ID = 0
      D1 = 0.0
      DO 3  J=1,M
        DO 3  I=1,N
3        X(I,J) = X(I,J) + BB(I,J)
C  COMPUTE NEW RESIDUALS
      DO 5  J=1,M
        XMAX = 0.0
        BBMAX = 0.0
        DO 4  I=1,N
          1 IF(ABS(X(I,J)),GT,XMAX)  XMAX = ABS(X(I,J))
          1 IF(ABS(BB(I,J)),GT,BBMAX)  BBMAX = ABS(BB(I,J))
          CALL INRPRO(N,-B(I,J),0.,A(I,1),IA,X(I,J),1,C,CC)
4        BB(I,J) = -C
          1 IF(BBMAX,GT,D1=XMAX)  D1 = BBMAX/XMAX
5        1 IF(BBMAX,GT,2.0*EPS*XMAX)  ID = 1
          IF(2.0*D1,GT,D0 .AND. L,NE.1)  ILL = L
          D0 = D1
          IF(ID,EQ,1)                      GO TO 2
      RETURN
      END

```

```

      SUBROUTINE PRNPLT(X,Y,XMAX,XINCR,YMAX,YINCR,ISX,ISY,NPTS)
C  PRINTER PLOT ROUTINE          M.S. ITZKOWITZ      MAY, 1967
C
C  PLOTS THE 'NPTS' POINTS GIVEN BY 'X(I),Y(I)' ON A 51 X 101 GRID
C  USING A TOTAL OF 56 LINES ON THE PRINTER
C  IF 'ISX' OR 'ISY' ARE NON-ZERO, THE CORRESPONDING MAXIMUM AND

```

```

C      INCREMENTAL STEP SIZE ARE COMPUTED
C      IF EITHER INCREMENTAL STEP SIZE IS ZERO, THE PROGRAM EXITS
C      NEITHER OF THE INPUT ARRAYS ARE DESTROYED, IF SCALING IS DONE
C      THE CORRESPONDING NEW VALUES OF MAXIMUM AND STEP SIZE ARE RETURNED
C
C      DIMENSION X(NPTS),Y(NPTS),IGRID(105),XAXIS(11)
C
C      INTEGER BLANK,DOT,STAR,IGRID,PLUS
C      DATA BLANK,DOT,STAR,PLUS / 1H ,1H,,1H*,1H+
C
C      901 FORMAT(14X,105A1)
C      902 FORMAT(1XE10.3,2X,1H+,105A1,1H+)
C      903 FORMAT(15X,103(1H,})
C      904 FORMAT(7X,11(F10.2),2H (,I4,5H PTS)  )
C      905 FORMAT(16X,11(1H+,9X))
C      9800 FORMAT(46H1SCALING ERROR IN PRNPLT, EXECUTION TERMINATED )
C
C      IF(XINCR.EQ.0..OR.YINCR.EQ.0.) GO TO 800
C      YAXMIN=0.01*YINCR
C      XAXMIN=0.01*XINCR
C      IZERO=YMAX/YINCR+1.5
C      JZERO=103.5-XMAX/XINCR
C      IF(JZERO.GT.103.0R.JZERO.LT.4) JZERO=2
C      PRINT 905
C      PRINT 903
C      DO 10 I=1,51
C      IF( I.NE.1ZFRO) GO TO 16
C      DO 14 J=1,105
C      14 IGIRD(J)=PLUS
C      GO TO 15
C      16 DO 11 J=1,1P5
C      11 IGIRD(J)=BLANK
C      15 IGIRD(JZERO)=PLUS
C      IGIRD(104)=DOT
C      IGIRD(2)=DOT
C      DO 12 K=1,NPTS
C      ITEST =(YMAX-Y(K))/YINCR+1.5
C      IF( ITEST .NE.1) GO TO 12
C      J=103.5-(XMAX-X(K))/XINCR
C      IF(J.GT.103) J=125
C      IF(J.LT.3) J=1
C      IGIRD(J)=STAR
C      12 CONTINUE
C      IF(MOD(I,1W).EQ.1) GO TO 13
C      PRINT 901,IGRID
C      GO TO 19
C      13 YAXIS=YMAX-(I-1)*YINCR
C      IF(ABS(YAXIS).LT.YAXMIN) YAXIS=0.
C      PRINT 902,YAXIS,(IGRID(J),J=1,105)
C      10 CONTINUE
C      PRINT 903
C      PRINT 905
C      DO 20 M=1,11
C      XAXIS(M)=XMAX-XINCR*(FLOAT(11-M))*10.0
C      IF(ABS(XAXIS(M)).LT.XAXMIN)XAXIS(M)=0.
C      20 CONTINUE
C      PRINT 904,XAXIS,NPTS
C      RETURN
C      800 PRINT 9800
C      END

```

Subroutine ADDVEC (vector addition) is called in BAND. Also, ADDVEC and Function DOTPRO (dot product) are used in BANS 1. These are in the LASL Subroutine Library. They are listed below:

```
SUBROUTINE ADDVEC(N, W, X, IX, Y, IY, Z, IZ)
DIMENSION X(1), Y(1), Z(1)
IF (N, LE, 0)                                RETURN
J = 1
K = 1
L = 1
DO 1  I=1, N
      Z(L) = W*X(J) + Y(K)
      J = J + IX
      K = K + IY
1      L = L + IZ
                                RETURN
END
FUNCTION DOTPRO(N, X, IX, Y, IY)
DIMENSION X(1), Y(1)
DOUBLE PRECISION D
IF (N, GT, 0)                                GO TO 1
DOTPRO = 0.
                                RETURN
1      D = 0.
J = 1
K = 1
DO 2  I=1, N
      D = D + X(J)*Y(K)
      J = J + IX
2      K = K + IY
DOTPRO = D
                                RETURN
END
```

ACKNOWLEDGMENTS

A number of people have contributed to this effort. I wish to acknowledge the valuable counsel of Professor Alan D. Randolph who has offered many valuable and detailed suggestions throughout the whole project. My thanks to Dr. Peter G. Salgado for his helpful suggestions in the design of the apparatus, to Dr. William A. Cook for his kind assistance with the mathematics and programming, to Dr. Michael Steuerwalt for his assistance in providing the numerical analyses and programming, and to Robert E. Smith for providing the scanning electron micrographs of the products.

I am happy to acknowledge the assistance and encouragement given me by my Committee on Studies: Dr. Robert H. Dinegar who also performed the test firing, Professor Fritz S. Allen, and Professor William F. Coleman.

My thanks to the technicians who assisted in the experimental work: Calvin C. Maxwell, Edward Velarde, Lee E. Naranjo, and Benjamin O. Martinez, and to the technicians who provided the particle size analyses: Francis V. Dare, Herman R. Roybal, Carlos A. Martinez, Donald E. Rickenbaugh, and Alfredo L. Ortiz. Finally, I am indebted to Eleanor L. Petrie for her painstaking care in typing the manuscript.

This work was performed at the Los Alamos Scientific Laboratory under the auspices of the Energy Research and Development Administration contract W-7405-ENG-36.

REFERENCES

1. Barlow, E.; Barth, R. H.; and Snow, J. E., The Penta-erythritols (Reinhold Publishing Corp., New York, 1958), p. 54.
2. Bor, T., "The Static Mixer as a Chemical Reactor," Br. Chem. Eng. (July 1971).
3. Cook, M. A., The Science of High Explosives (Reinhold Publishing Corp., New York, 1958), p. 1.
4. Danckwerts, P. V., "Continuous Flow Systems," Chem. Eng. Sci. 2, 1 (1953).
5. Davis, T. L., The Chemistry of Powder Explosives (John Wiley and Sons, Inc., New York, 1943), pp. 278-281.
6. Dixon, W. J., and Mood, A. M., "A Method for Obtaining and Analyzing Sensitivity Data," J. Am. Statist. Ass. 48, 109 (1953).
7. DuBois, F. W., and Baytos, J. F., "Photelometer Method for Particle Size Measurement Using Improved Dispersing, Recording, and Computing Techniques," Los Alamos Scientific Laboratory internal report (April, 1968).
8. Hamming, R. W., Numerical Methods for Scientists and Engineers, 2nd Ed. (McGraw-Hill Book Company, New York, 1973).
9. Hatler, L. E., "Continuous Crystallization of High Explosives," Los Alamos Scientific Laboratory report LA-5235-MS (April 1973).
10. Hulbert, H. M.; and Katz, S., "Some Problems in Particle Technology," Chem. Eng. Sci. 19, 555 (1964).
11. Hutchinson, R. W.; Kleinberg, S.; and Stein, F. P., "Effect of Particle-Size Distribution on the Thermal Decomposition of α -Lead Azide," J. Phys. Chem. 77, 870 (1973).
12. Kenics Corporation Bulletin No. SM5.
13. King, D. R.; and Panowski, J. B., "Determination of Particle Size Distribution and Surface Area by Photometry," Los Alamos Scientific Laboratory report LA-1267-MS (May 1948).

14. McCormick, J. M.; and Salvadori, M. G., Numerical Methods in FORTRAN (Prentice-Hall, Inc., Englewood Cliffs, NJ, 1964).
15. Levenspiel, D., Chemical Reactor Engineering, 2nd Ed. (John Wiley and Sons, Inc., New York, 1972), p. 272.
16. Randolph, A. D., and Larson, M. A., "Transient and Steady State Size Distributions in Continuous Mixed Suspension Crystallizers," AICHE J. 8, 639 (1962).
17. Randolph, A. D.; and Larson, M. A., Theory of Particulate Processes (Academic Press, New York, 1971), Chaps. 2 and 3.
18. Reynolds Industries, Inc., EBW Explosive Products (Marina del Rey, CA).
19. Roberts, R. N.; and Dinegar, R. H., "Solubility of Pentaerythritol Tetranitrate," J. Phys. Chem. 62, 1009 (1958).
20. Scott, C. L., "Effect of Particle Size on Shock Initiation of PETN, RDX, and Tetryl," The 5th Symposium on Detonation, Pasadena, August 18-21, 1970, 148 (ONR report DR-163, 1970).
21. Southworth, R. W., and Deleeuw, S. L., Digital Computation and Numerical Methods (McGraw-Hill Book Co., New York, 1965).
22. Tucker, T. J., "Explosive Initiators," 12th Annual Symposium on Behavior and Utilization of Explosives in Engineering Design, University of New Mexico, Albuquerque, March 2-3, 1972, 175 (New Mexico Section of the American Society of Mechanical Engineers, 1972).
23. Wehner, J. F., and Wilhelm, R. H., "Boundary Conditions of Flow Reactor," Chem. Eng. Sci. 6, 89 (1956).